Final Report

Award Number: DE-EE0008724

FOA FOA Topic Area: Solid-State Lighting Advanced Technology R&D – 2018
FOA Topic 3: Advanced Fabrication R&D
Subtopic: OLED Substrate and Encapsulation Fabrication
DE-FOA-0001823

Name of Recipient: Iowa State University

Project Title: "Enhanced Light Outcoupling from OLEDs Fabricated on Novel Low-Cost Patterned Plastic Substrates of Varying Periodicity"

PI: Ruth Shinar

Team Members:
Ruth Shinar, Joseph Shinar (co-PI), Rana Biswas (co-PI); graduate students: Rajiv Kaudal, Erik Dykstra, Michael Fralaide, Yu Zhang - Iowa State University;
Dennis Slafer - MicroContinuum, Inc. (Watertown, MA)

Date of Report: January 31, 2022

Contact: Ruth Shinar
Phone: 515-294-5898
Email: rshinar@iastate.edu

SSL Project Manager: Joel Chaddock -

Executive Summary

OLEDs continue to make strides in display applications, but their commercial utilization in solid-state lighting (SSL) is lagging. An ongoing challenge, in particular for manufacturing, is the need for enhanced efficiency and hence the necessity to increase in an inexpensive approach the extraction of the light generated inside the OLED into the forward (viewing) hemisphere. In conventional OLEDs fabricated on a transparent flat anode coated on glass, the external quantum efficiency (EQE) is only ~20%. About 50% of the light is lost to internal waveguiding in the high refractive index (RI) organic + ITO anode layers and to surface plasmon polaritons (SPPs) at the organic/metal cathode interface. Another ~30% of the light is externally waveguided in the substrate to its edges. While extraction of the externally waveguided light is commonly addressed by adding a microlens array (MLA) or a scattering layer at the substrate's air-side, light outcoupling increases by only ~1.6-1.7x (*vs* up to 2.5x in improving from ~20% to ~50%). The use of a hemispherical lens or an index matching fluid (IMF) at the substrate/photodetector (PD) interface increases the outcoupling by at least 2x; these approaches however, are not viable industrially, and even a MLA is sometimes undesirable due to its non-planar, scattering structure. In multi-stack tandem OLEDs, where the metal cathode is far from the emitting zone(s), the impact of photons loss to SPPs decreases.

Our project addressed the ~50% loss to the internally waveguided light and SPPs. We evaluated OLEDs fabricated on patterned or planarized plastic substrates manufactured in a cost-effective approach compatible with a roll-to-roll (R2R) process. The OLEDs were either (*i*) patterned to various degrees depending on the pitch *a* and height or depth *h* of the pattern features or (*ii*) planar, with a pattern buried under a flat high RI planarization layer.
We demonstrated that the outcoupling from green patterned OLEDs reaches ~50% by mitigating plasmon–related loss and internal waveguiding, even without the addition of a MLA, a hemispherical lens, or IMF. Simulations conducted in parallel with the experimental effort demonstrated how diffraction by conformally corrugated OLEDs increases the outcoupling to >60%. Structures with varying pitch values were also simulated indicating that combining domains of varying pitch could increase outcoupling to 55-60%.

Experimentally, we additionally assessed the role *a* and *h* in determining not only the OLED efficiencies, but also their structural properties, i.e., the uniformity and conformality throughout the OLED stack.

As planar OLEDs are preferred over corrugated devices, we studied different patterns in plastic substrates that were planarized by a high RI formulation. Planar green OLEDs on such structures showed enhanced efficiencies with EQEs larger than 60% with the addition of an IMF (to extract the substrate mode) at the substrate/Si PD interface. White OLEDs showed EQEs of 45.5%.

Plastic substrates are currently less attractive than glass substrates due to drawbacks such as permeability to water vapor and oxygen, and in some cases thermal instability. Plastic substrates however, are flexible and easy to handle unlike thin flexible glass, and once transparent thin barrier films are available, they will become more attractive; they are already of interest in medical applications. Importantly, as it is easy to generate various patterns in different plastic materials, they provide excellent means for assessing and optimizing enhancing extracting structures. Such structures can also be transferred to glass substrates with some process modifications.

The technical effectiveness and economic feasibility of the project lie in the patterning of the extracting plastic substrates in an approach that is scalable to R2R manufacturing. R2R processes are of drastically lower-cost than batch or single-unit fabrication. The patterned plastic can be a part of an integrated substrate either plastic or glass, which includes also a

MLA or a planar layer with embedded scattering particles, as well as a conductive metal mesh/electrode design.
SSL is environmentally-friendly and as OLED SSL becomes more efficient it will reduce electricity consumption, and hence lighting cost, as well as produce less expensive attractive lighting fixtures. Our university-industry collaboration is hence of major benefit to the public as it demonstrates the feasibility of manufacturing optimized extracting substrates for highly efficient OLEDs for SSL in a future R2R process, which would drastically reduce the manufacturing cost and increase production in the USA. Moreover, newly developed methods by our team allow low-cost roll manufactured substrates to be transferred to flexible or rigid glass substrates, which solves the plastic substrate barrier issues, and when combined with device encapsulation will increase the OLEDs' environmental stability.

Accomplishments & Milestones

(Achieved milestones are marked throughout the text and a Milestone Summary Table is provided at the end of the section)

Project Objectives

The overall goal of the project was to achieve a light outcoupling factor η_{out} approaching 70% in phosphorescent OLEDs using novel extracting substrates whose fabrication is transferrable to a low-cost R2R process. The new substrates had patterns of varying pitch and height, including smooth single-period ordered & random multiple-period structures. They were convex or concave and of different materials, such as polycarbonate (PC), polymethyl methacrylate (PMMA), or polyethylene terephthalate (PET). OLEDs on planarized plastic substrates, i.e., substrates with buried patterns, similar to or reminiscent of MLAs, which are planarized with a high RI layer, were also evaluated

To achieve this goal we:

(1) Fabricated single-period corrugated substrates (Year 1 + continued in year 2) with smooth features devoid of sharp edges.
   (*i*) Fabricated patterned OLEDs on such substrates with varying pitch (i.e., period) *a* and height *h* (eventually with added IMF to replace less efficient MLAs); the anodes were ITO or PEDOT:PSS. Convex & concave designs, as well as planarized structures were evaluated.
   (*ii*) Fabricated semi-flat and planar OLEDs. Partially flattened OLEDs were fabricated on relatively shallower corrugations of feature heights $h < 200$ nm. Planar devices were fabricated on substrates with buried corrugations planarized by high RI coatings at a suitable thickness. Structures with an additional MLA to extract the substrate mode, or a top pattern so that the substrate is dual-patterned were also designed.
(2) Fabricated complex, random or multiple-period corrugated plastic substrates (Year 2). Ordered and complex substrates with (quasi) random period distributions were evaluated for both patterned and plane OLEDs.
(3) Optimized substrates for tandem OLEDs (Year 2) on corrugated and planarized substrates. Tandem devices were planned to be fabricated and evaluated at OLEDWorks. For this purpose, we need to transfer the structures to glass substrates and enable device encapsulation; this has been demonstrated at MicroContinuum Inc. (MCI).
In addition to characterizing OLEDs by measuring the electroluminescence (EL) spectra, *J-L-V* characteristics, efficiencies, etc., we evaluated the conformality of the patterned OLED stack. We used focused ion beam (FIB) analysis and edge SEM imaging to assess the conformality in relation to *h, a,* and *a*/*h*, including the effect of these parameters on η_{out} and general device performance on convex, concave, and planarized structures.

We explored two main substrate structures: (*i*) a single material with a directly imprinted top pattern (in e.g., PC, PMMA) and (*ii*) a two-layer structure of a planar base (e.g., PET) with a second patterned top layer (e.g., cellulose acetate butyrate, CAB, or UV acrylate). Both substrate types, whether with convex or concave nano-arrays, have been integrated with transparent conductors (TCs), including smooth (no raised metal step) metal meshes that will enhance the conductivity, and a MLA or a scattering layer at their air-side.
(4) Performed substrate and OLED design simulations to guide the experiments and predict the maximal achievable outcoupling of patterned and planar devices with diffracting and scattering patterns (Years 1 & 2).

Background and Approach: The fraction of light generated in an OLED that is emitted in the forward direction, i.e., the extraction or outcoupling factor η_{out}, is only ~20% in conventional bottom-emitting OLEDs. This is due to internal waveguiding resulting from total internal reflection (TIR) at the anode/substrate interface and surface plasmon-related losses that add to a combined >50% loss of outcoupled light; an additional ~30% of the light is waveguided through the flat substrate to its edges ("external waveguiding"). While partial extraction of the externally waveguided light via, e.g., MLAs, is now standard practice, minimizing the internally trapped light and plasmon-related losses without adversely affecting the OLEDs' attributes and in a cost-effective approach has proven to be challenging.

This project aimed to increase the outcoupling from OLEDs via use of innovative extracting, integrated plastic substrates. These included corrugated substrates and planar substrates with a buried pattern planarized by a high RI layer. These structures were of various designs that are easily fabricated in different materials using a low-cost imprint process compatible with R2R or batch processing. The structures reduce internal waveguiding and losses to SPPs. We achieved very encouraging results of outcoupling enhancement for OLEDs formed on corrugated substrates without MLAs, a hemispherical lens, or the use of an index matching fluid (IMF), all of which further increase η_{out}. In particular, addition of an IMF at the substrate/photodetector (PD) interface resulted in increased EQE >50% for patterned OLEDs and an EQE exceeding 60% for a green and 45.5% for white planar OLED on planarized extracting substrates (PES). An important aspect of the integrated substrates was improving the anode, for which we tested a thin Cu mesh conformally embedded in the substrate. Development of such an embedded mesh in the patterned substrate was challenging. We successfully generated a metal mesh in the high index planarization layer coating a buried pattern, which is very promising for further improving the OLEDs, and particularly desirable by panel manufacturers.

We note that since the internal quantum efficiency (IQE) cannot be measured directly neither can η_{out} = EQE/IQE, so any determination of η_{out} is model-dependent; the only model-independent conclusion on η_{out} is that it is obviously ≥ EQE.

Results and Accomplishments:

The project was performed at Iowa State University (ISU) and MCI.

Enhancing Substrates

MCI's fabrication of the corrugation is based on two approaches:
(1) *Direct substrate nanopattern formation* (proprietary): with this approach there are no interfaces, hence peel off issues are eliminated as well as index mismatch losses. The fabrication is at room temperature, avoiding thermal distortion /degradation. This approach

reduces production time, eliminating slow heating/cooling cycles, and is suitable for various materials and adjusting pattern heights without the need for costly new templates.
(2) *Custom radiation cross-linked polymer formulation*: with this approach, the pattern and the substrate are independently optimized and the refractive index can be adjusted by monomer modification and addition of high index particles to extract the externally waveguided photons via scattering by the high RI particles.

Substrate Types
We demonstrated two types of enhancing substrates**:** (*i*) fully integrated substrates with a smooth top corrugation, devoid of sharp edges (**Milestone 1**). Such integrated substrates included a metal mesh embedded into the corrugation underneath a thin ITO layer. OLEDs fabricated on such substrates, often presented shorts likely stemming from areas of protruding metal. These issues can be addressed by further refinement of the process. (*ii*) planarized extracting substrates (PES) (**Milestone 10**) are designed to avoid the shorting described above. Here, a buried pattern in a plastic substrate is planarized with a high RI layer so that the OLED is planar, which is the desired situation. We successfully embedded a Cu mesh in a high RI layer planarized over a buried low refractive index extraction pattern, forming a smooth, planar surface for OLED deposition. This is very promising for planar OLED EQE enhancement, particularly for panel manufacturing. Fig. 1 presents a few examples of corrugated substrates and a schematic of the fully integrated corrugated structure. Fig. 2 shows examples of PES, schematics of fully integrated PES, and a successfully embedded Cu mesh (**Milestone 3**) in the high RI of the planarizing layer of PES. This structure is expected to result in OLEDs with EQEs approaching 70% (**toward MS 13**).

With the fabrication process in hand, successful OLEDs on different PES were evaluated. To extract the substrate mode an IMF at the substrate/Si PD interface was employed. The IMF is more efficient than a MLA in extracting the externally waveguided light.

Anode Improvement (**MS 3**)
We often used successfully PEDOT:PSS as the anode. The PEDOT:PSS was treated with ethylene glycol to increase its conductivity, but it was still lower than that of ITO. We improved the PEDOT:PSS anode by embedding silver nanowires (Ag NW). We tested sheet resistance, transmission, and surface roughness of several PEDOT:PSS-Ag NW anode structures. The most promising structure in term of the above-mentioned attributes are sandwich structures of PEDOT:PSS/Ag NWs/PEDOT:PSS with the PEDOT:PSS on top, as its surface is relatively smooth (~4-5 nm roughness) unlike that of the Ag NWs. The best sheet resistance was 50 Ω/□. The transmission in the green is ~93% somewhat lower than that of PEDOT:PSS (95-96%). The ITO is still preferred, as spin coating appears to lead to non-uniform deposition, depending on the pattern parameters. As shown later, we used such a spin-coated layer to generate complex structures.

ITO deposition
Following experiments to optimize the ITO, we obtained smooth layers of ~2-3 nm surface roughness with the best sheet resistances of ~25 to 50 Ω/□. A transfer process depicted in Fig. 3 was developed at MCI for achieving such smooth surfaces. The ITO was deposited first on a smooth, flat PET substrate having a thin (<10 nm) PTFE release layer that served as a donor sheet. As the thickness of the ITO increases, so does its growing surface roughness. The ITO was then transferred to a receiving PET substrate coated with a thin bonding layer. As a result, the top ITO surface on which the OLED is fabricated had a low surface roughness mirroring that of the original PET donor film. Moreover, high quality ITO on PES was achieved by the transfer

technique using ITO deposited on a PET donor film at room temperature and under very low inert gas background pressure.

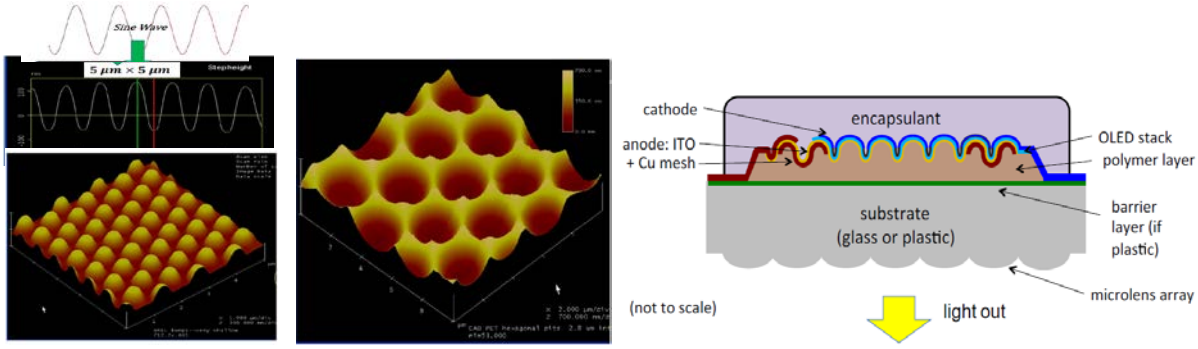

Sinusoidal PC
***h* ~200 nm**
***a* ~780 nm**

PET/CAB
***a* ~2.8 μm**
***h* ~500 nm**

Fig. 1. *Left: AFM images and section analysis of PC and PET/CAB corrugated substrates. Right: schematic of the fully integrated patterned structure.*

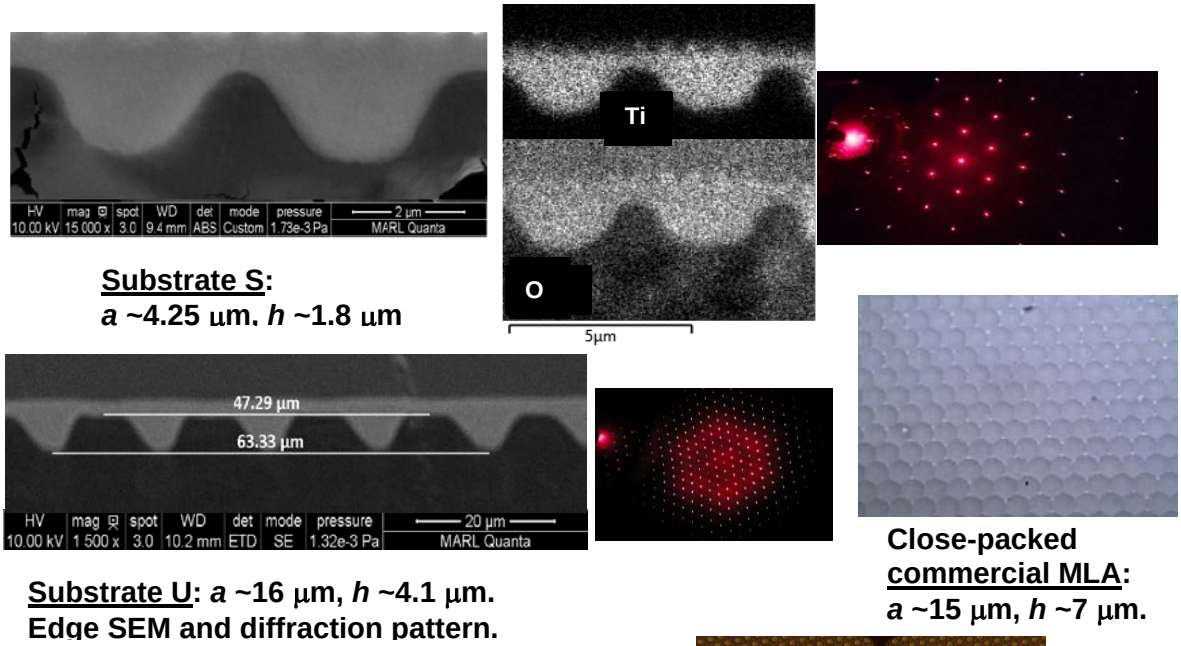

Substrate S:
***a* ~4.25 μm, *h* ~1.8 μm**

Substrate U: ***a* ~16 μm, *h* ~4.1 μm.**
Edge SEM and diffraction pattern.

Close-packed commercial MLA:
***a* ~15 μm, *h* ~7 μm.**

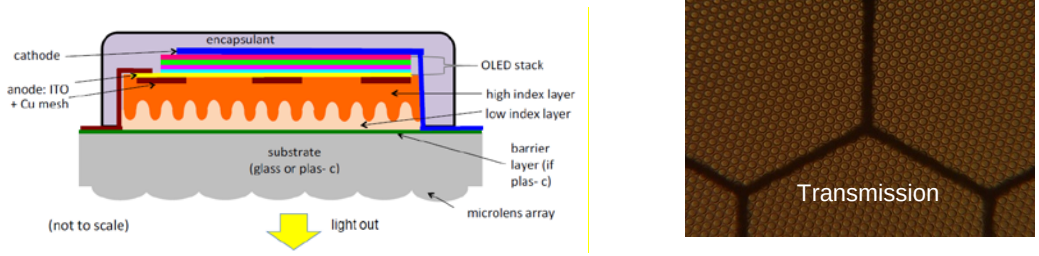

Fig. 2. *Edge SEM & diffraction patterns of Substrate S (top) and Substrate U (center left); laser diffraction pattern of closed-packed commercial MLA (Center right); OLED/PES schematics & optical image of Substrate S + Cu mesh embedded in a high RI planarizing layer (Bottom).*

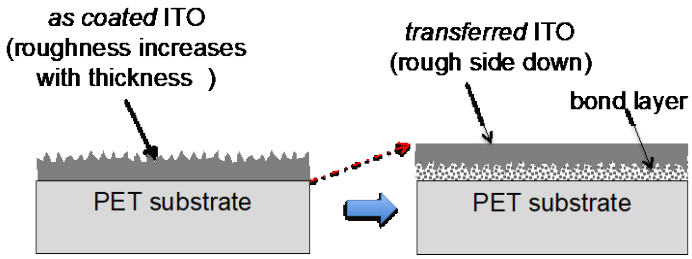

Fig. 3.*Schematics of the transfer process used for deposition of smooth ITO.*

Development of a Buried Metal Mesh

We previously reported the successful fabrication of an embedded mesh in planar plastic with light transmission >99.5%; this was achieved for a Cu mesh with 750 nm wide lines with a 200 µm pitch in a 2 mil PET substrate. As with ITO deposition, we recently successfully used the metal mesh transfer process shown in Fig.4. Furthermore, we recently successfully generated a planar metal mesh embedded in a high RI planar layer over an extraction pattern in a lower RI plastic (see Fig. 2). As shown below, OLEDs on such PES present enhanced EQEs of ~61% for a green OLED and 45.4% for a white OLED (WOLED).

The fabrication of a conformal buried mesh in a corrugated substrate is more challenging as any protruding metal will result in shorts in the OLEDs, as mentioned above.

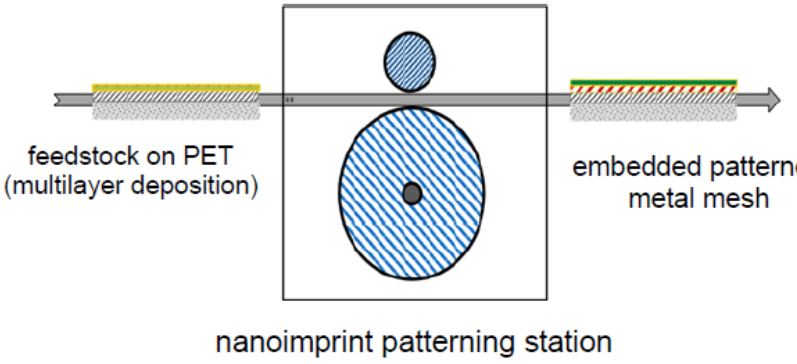

Fig. 4. *R2R process step* (non-proprietary) *of forming a metal mesh pattern buried under a continuous ITO layer, using UV nanoimprint processing.*

Substrate Mode Extraction: Air-side MLAs (**MS 4**)

We fabricated successfully MLAs at the airside of corrugated substrates. MLAs included those fabricated by imprinting a mold generated by UV laser interference lithography into polyurethane (PU) that was successfully attached to the plastic substrate, commercial MLA, and MLAs fabricated directly into the airside of top corrugated plastic substrates. An example of an embedded MLA is shown in Fig. 5. In a novel approach, the MLA was embedded within a high index NOA170 (n ~1.7; Norland product), which then led to the formation of PES. In this example, the structure included additionally a shallow top corrugation (dual pattern **MS 7**). However, such dual structures need optimization.

Using such MLAs resulted in mixed results. We typically observed enhancements that were significantly lower than those achieved by using IMF at the substrate/Si photodiode (PD) interface. In other cases while we saw increased EQEs with corrugated OLEDs, the addition of a PU MLA to a corrugated OLED showed a similar EQE to that of a reference planar OLED with an embedded MLA. The latter result indicates that the embedded MLA may work better than the attached PU one, as a 35% increase in the EQE was observed for the top corrugated OLED (with no MLA). The different MLAs we used and some results are presented in Fig. 5.

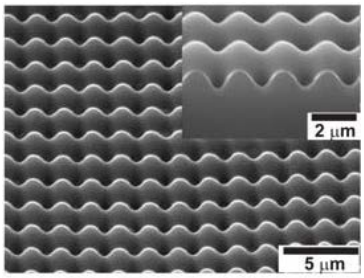

a =2 μm; *h* ~1 μm

PU MLAs generated by a mold fabricated by UV laser interference lithography.

a ~1.85 μm, *h* ~850 nm

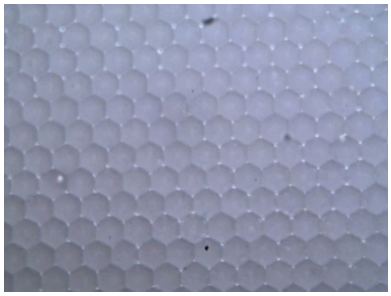

Optical image of a close-packed commercial MLA: *a* ~15 μm, *h* ~7 μm.

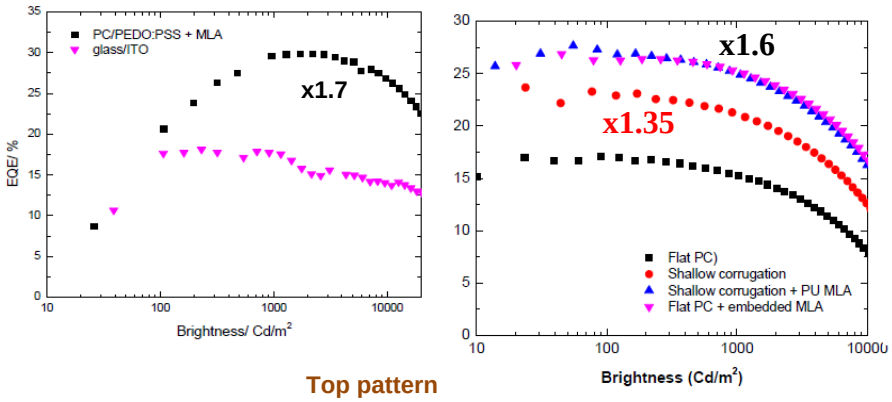

Top pattern

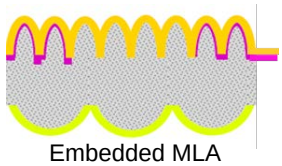

Embedded MLA

Enhanced green OLED with the attached PU MLA of *a* ~1.85 μm & *h* ~850 nm. The PC substrate was of *h* ~55 nm & *a* ~750 nm & the anode was PEDOT:PSS.

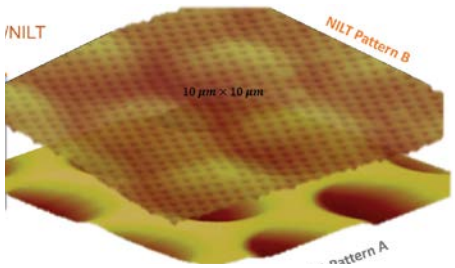

MLA

Fig. 5. *Top: different MLAs used for enhancing the substrate mode outcoupling. Center: enhanced outcoupling of 70% using a commercial MLA at a planar PC/OLED (left); enhanced corrugated OLED with a PU MLA (center), and schematic of an embedded MLA (right) used with the reference flat PC.* Bottom: AFM images of a dual corrugated substrate: top corrugation: *a* ~370 nm, *h* ~50 nm & a buried MLA: *a* ~4 μm, *h* ~1 μm.

Following these results, we resorted to the use of an IMF, which presents a better measure for the extracted internally waveguided light into the substrate and mitigation of SPPs.

Enhanced OLEDs

None of the OLEDs studied were encapsulated. Some OLED pixels showed slopes of e.g., increasing EQE at low current densities. This situation is believed to be due to local defects, contaminations, or device deterioration during the measurements. It is possible that filamentary shorts that burn out at higher voltages are responsible for this profile.

Effect of Corrugation Height & Pitch for achieving EQE ~45% (**MS 2**)
We continued with performing systematic studies of changing the corrugation pitch and height for pattern optimization. Patterned substrates with *a* ranging from ~275 nm to 7.8 μm and *h* ~50 to 500 nm were evaluated; some examples are provided below. Fig. 6 shows enhanced EQEs of green OLEDs on substrates with *h* ~80 nm and *a* 275 nm (Motheye) and 750 nm. The device structure on the Motheye substrate was:

PEDOT:PSS/HAT-CN(5 nm)/10% MoOx:TAPC(*x*)/TAPC(20 nm)/6% Ir(PPy)$_3$:mCP (20 nm)/TmPyPb (35 nm)/LiF (1 nm)/Al (100 nm); *x* = 25, 30, 35, 40 nm,
with x = 35 nm providing the optimal results.

An EQE of ~37%was achieved, a 70% increase relative to a planar reference.

The optimized device structure on the substrate with *a* ~750 nm was:
PC/PEDOT:PSS/HAT-CN (5 nm)/10% MoOx:TAPC (60 nm)/TAPC (20 nm)/6% Ir(ppy)$_3$:mCP (20 nm)/TmPyPb (20 nm)/20% CsF:TmPyPb (40 nm)/LiF (1 nm)/Al (100 nm).

A similar EQE of ~40% was achieved, a 90% enhancement.

For green OLEDs we achieved EQEs of ~48% to 50% for optimized devices with *a* ~750 nm and *h* ~165 nm to 320 nm, typically a 2x enhancement relative to a planar device on plastic. A green OLED on a substrate with *h* ~500 nm and *a* ~1.9 μm showed a lower EQE of ~30%, 1.7 x enhancement. For blue and white OLEDs on substrates with *a* ~750 nm, the EQEs we obtained were ~34% as shown in Figs. 7 and 8. Examples of EQEs of green OLEDs are also shown in Fig. 7 and rigorous simulations predicting the effects of *h* and *a* in corrugated OLEDs follow.

The structure of the white OLED was:
PC-280/PEDOT:PSS (~20 nm)/HAT-CN (5 nm)/10% MoOx:TAPC (120 nm)/TAPC (20 nm)/8% FIrpic:mCP (19 nm)/6% PO-01:mCP (1 nm)/TmPyPb (20 nm)/20% CsF:TmPyPb (40 nm)/LiF(1 nm)/Al (100 nm).

The substrate was of *h* ~280 nm & *a* ~750 nm and the EQE was 32%. As shown below, *h* reduced to ~200 nm at the Al cathode.

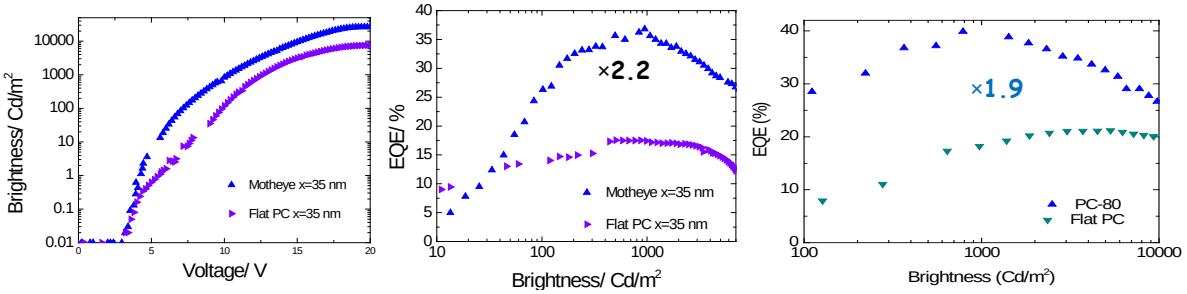

Green OLEDs on flat & patterned PC
h ~80 nm & *a* ~275 nm

Green OLEDs on flat & patterned PC
h ~80 nm & *a* ~750 nm

Fig. 6. *Comparison of pitch effect on the EQE of patterned OLEDs fabricated on PC substrates with h ~80 nm and of 275 nm and 750 nm.*

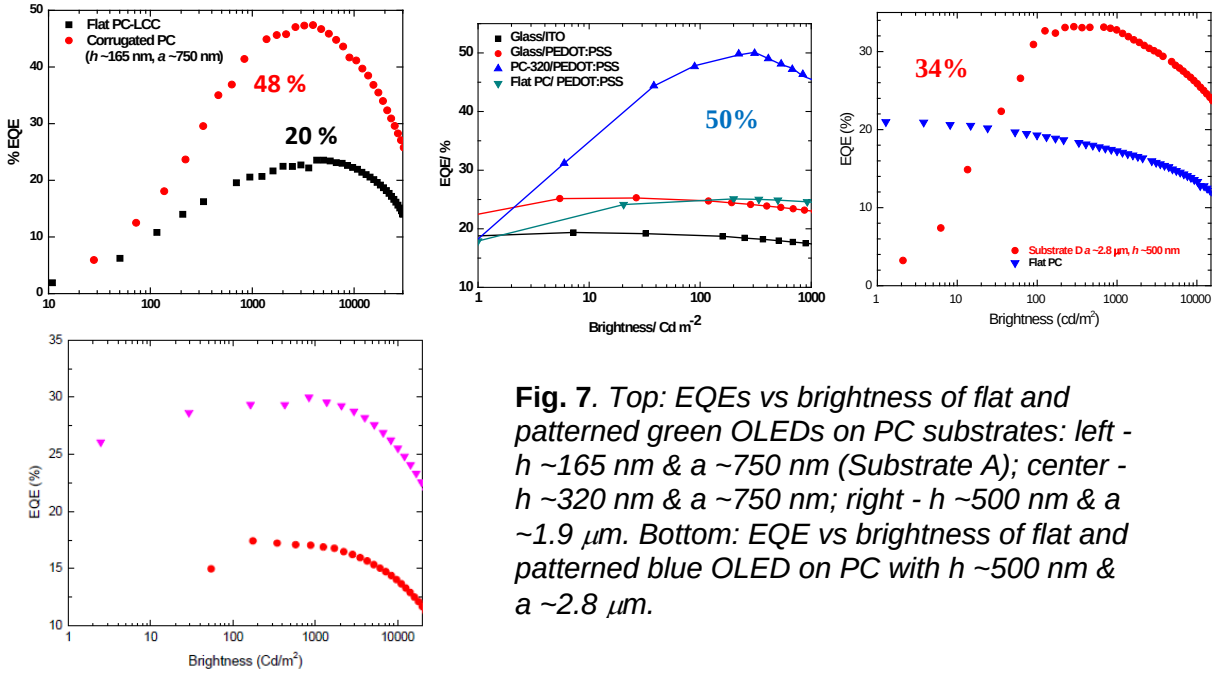

Fig. 7. *Top: EQEs vs brightness of flat and patterned green OLEDs on PC substrates: left - h ~165 nm & a ~750 nm (Substrate A); center - h ~320 nm & a ~750 nm; right - h ~500 nm & a ~1.9 μm. Bottom: EQE vs brightness of flat and patterned blue OLED on PC with h ~500 nm & a ~2.8 μm.*

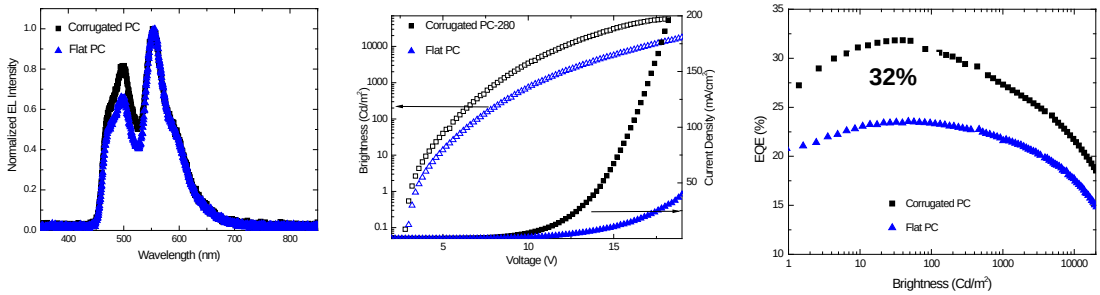

Fig. 8. *Attributes of a white OLED on A PC substrate of h ~280 nm & a ~750 nm*

The simulations assume conformal OLEDs, however experimentally the OLED stack conformality varied depending on *a & h* as shown below. The effect of the non-conformal stack requires further evaluation, as the EQE enhancement did not show a clear dependence on the corrugation variation as the OLED was built.

Advanced scattering matrix method: corrugated OLEDs (MS 1)

We have developed the advanced scattering matrix method to simulate the light emission from corrugated OLEDs. Here Maxwell's equations are solved in *Fourier* space – which is a major advantage to simulating thick substrates. In contrast, real space methods consume large memory in simulating thick substrates. In this method the experimental values of the complex refractive indices $n(\lambda)+ik(\lambda)$ for each layer material are adopted. The ***E*** and ***H*** fields within the different OLED layers and in air are simulated. The dipole source in the emissive layer is also conformally corrugated (Fig. 9) - a complexity not present in flat OLEDs. In our algorithm, we utilize the Purcell enhancements at the dipole location. We utilize all 3 polarizations of the dipole were utilized (x, y, z), corresponding to TMh, TEh and TMv polarizations (h: horizontal; v: vertical). For each polarization (j) of the dipole we simulate the spectral power emitted inside OLED $P_{in}(k_{||})$ and the spectral power emitted to air $P_{out}(k_{||})$, where $(k_{||})$ is the parallel light

wavevector. By integration over $k_{||}$ and sum over the polarizations, we find the total power emitted inside P_{tot} and outcoupled to air P_{air}.; the ratio of these powers provide the outcoupling $\eta_{out} = P_{air}/P_{tot}$.

$$\eta_{out} = \frac{\sum_{j=1}^{3} P^{air}(j)}{\sum_{j=1}^{3} P_{tot}(j)} \qquad (1)$$

In general, available commercial software work very efficiently for flat OLEDs but are difficult to adapt for corrugated OLEDS. This illustrates the advantages of our computational approach.

We simulate the outcoupling η_{out} as a function of the corrugation pitch *a* and height *h*, for three representative wavelengths: 610 nm (red), 530 nm (green), and 470 nm (blue) (Figs. 10 & 11). Since the optimum ETL thickness is a near a quarter wavelength $\lambda/4n(org)$, we calculate η_{out} for a range of ETL thickness around this value(~20 nm). For green OLEDs (λ=530nm, *n(org)* ~1.76) the value $\lambda/4n(org)$ is 75 nm. All the layers of the conformal OLED have corrugations of the same height, resulting in a complex three-dimensional emissive region that follows the corrugation contour. The OLED stack is polycarbonate (PC; *n*=1.58)/corrugations in PC (*h nm*, a)/HTL (*d(HTL)* nm)/emissive region/ETL *d* nm/Ag cathode (Fig. 9).

We show results for a constant corrugation *h*=200 nm. Since the triangular lattice of corrugations is anisotropic, it was necessary to simulate different planes for the light emission. Accordingly, we selected the parallel component of the photon wave-vector $k_{||}$ along the i) *x*-axis ii) *y*-axis, and iii) line 45° to the *x* and *y* axis, corresponding to light emission in the *xz*, *yz* planes, and the plane bisecting *xz*, *yz* planes, respectively. We initially selected the dipole emission from the ring-like contour closest to the substrate ('low' position).

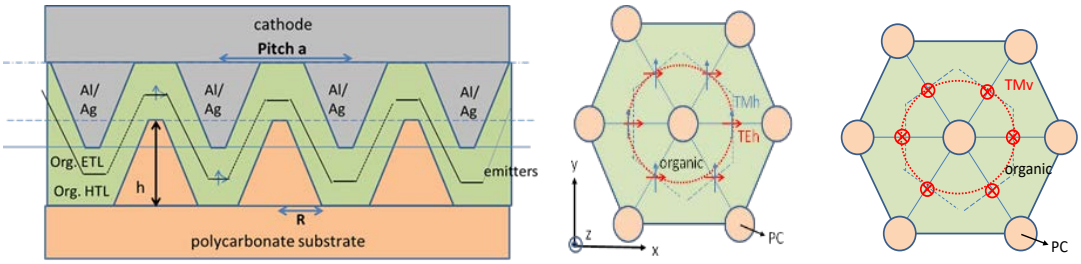

Fig. 9. *Left: Schematic structure of the corrugated OLED in a two-dimensional projection. Right: Dipole emitters positions in a planar x, y OLED cross section; the horizontal polarizations of the dipole (TMh, TEh) and the vertical polarization (TMv).*

For each $k_{||}$, our simulation shows a broad maximum η_{out}~ 0.6-0.65 for pitch *a*~ 1000-2500 nm (Fig. 10). This provides an enhancement factor >3 from the flat OLED, where η_{out} ~0.2. We averaged the orientations to estimate the averaged η_{out} (Fig. 11).Simulations show optimal η_{out} ~0.6-0.65 for *a* ~1000-2500 nm. At large *a*, η_{out} decreases smoothly towards the flat limit (η_{out} ~0.2). For all three wavelengths η_{out} decreases sharply at smaller pitch *a*<500 nm, also approaching the flat OLED limit.

Plasmonic losses are sharply reduced by the corrugations, and are 5-10%. The waveguiding losses are ~30% near the optimal *a* (1-2.5 μm), but increase significantly at larger *a*, and increase sharply at small *a*<500 nm. At large *a*, as the corrugated structure approaches the flat limit, the predominant losses are from waveguided modes (70%) and smaller plasmonic loss (~10%), approaching the flat η_{out} ~0.2.

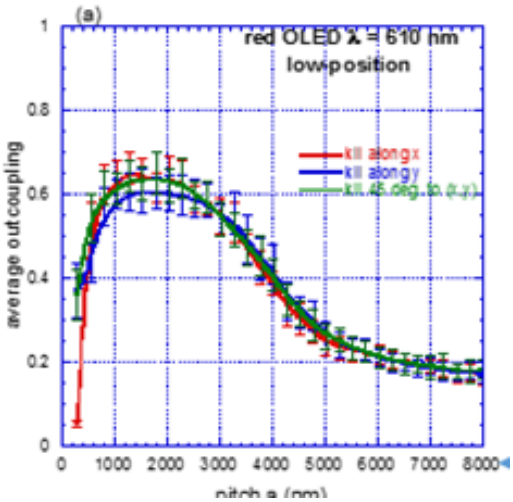

Fig. 10. *Simulated corrugated OLED outcoupling as a function of corrugation pitch a, for a fixed corrugation height h of 200 nm and a red wavelength of 610 nm. The parallel wave-vector $k_{||}$ is along x, y, and 45° to x or y axes,*

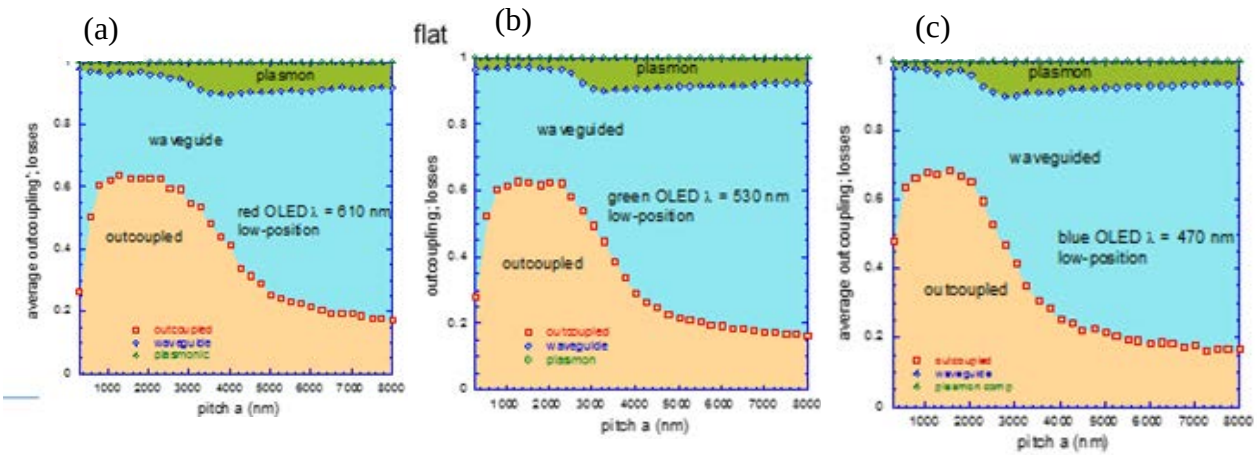

Fig. 11. *The average outcoupling is taken over ETL thickness d(ETL) from 60-80 nm to obtain the division of power into outcpoupled modes, waveguided modes and plasmonic losses for a) red wavelengths at 610 nm b) green OLEDs at 530 nm and c) blue OLEDS at 470 nm. The dipole emitter is in the low (L) position shown in Fig. 9.*

When *h* is varied (near optimal pitch *a*=1000 nm), η_{out} as well as waveguiding/plasmonic losses, are relatively insensitive to *h* (*h*>100 nm) for blue or green OLEDs (Fig. 12). The diffraction of waveguided and plasmonic modes into the air-cone is insensitive to *h*, which is highly beneficial for experiments - since small experimental variations in *h* should not influence η_{out}.

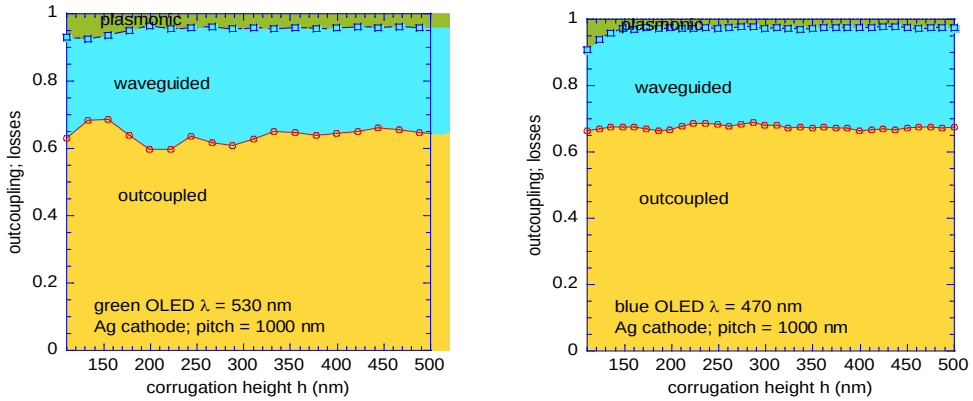

Fig. 12. *The division of power into outcoupled, waveguided and plasmonic losses for green (λ=530 nm) and blue (λ=470 nm) OLEDs as a function of h, from 100 nm to 500 nm for the low position (L).*

We show emission cones for a green OLED near the optimal *a*=750 nm in Fig. 13. First-order diffraction through $\mathbf{G}_1$, $\mathbf{G}_2$ vectors have the right magnitude to diffract waveguided and plasmon modes back to the air cone for emission in the *xz* plane ($k_{||}$ along *x*), and *yz* plane ($k||$ along *y*), indicating more isotropic emission, confirmed by the numerical outcoupling results.

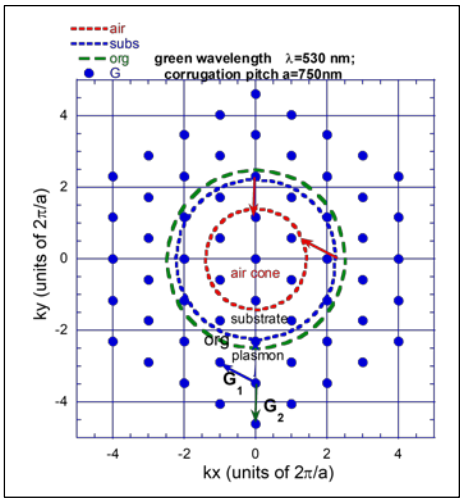

Fig. 13. *Reciprocal lattice of the triangular array (blue circles) with the primitive reciprocal lattice vectors* $\boldsymbol{G_1}$, $\boldsymbol{G_2}$ *is shown. Superimposed on this scale are the air emission cones for air, substrate, organic, and plasmon. First order diffraction is shown.*

<u>*OLED Stack Conformality on Patterned OLEDs: partial planarization*</u> (**MS 5 & MS 9**)
Previously we focused on relatively tall patterns with *h* ~300-400 nm. In this project we designed the new proposed plastic substrate templates that were smooth, single period (**MS 1**) including some with *h* <200 nm and *a* ~400 nm or ~750 nm. We used FIB analysis to gauge the conformality of the OLED stack. AFM imaging and section analysis of the substrates was used to monitor *h* before and after PEDOT:PSS application and to view the top of the completed device, i.e., at the Al cathode. We analyzed the efficiency enhancements in terms of the pitch-to-height ratio (*a*/*h*), but to test for a trend in the reduced *h* across he OLED stack additional studies with substrates of many more designs of varying *h* and *a* are needed. As shown below, in some cases the corrugation decreased significantly at the top Al cathode.

As seen in Fig. 14, the new shallow substrates, imaged by AFM, were largely devoid of sharp edges, including after spin coating the ~30-35 nm thick PEDOT:PSS anode. This study of shallow patterns was done in part to elucidate the conformality of the OLED layers fabricated on different patterns. Indeed, we showed using FIB analysis that with the relatively shallow *h*, fabricated OLEDs were gradually semi-flattened (i.e., with significantly reduced features' height at the top of the complete device).

FIB analysis of the complete OLED on Substrate A (Maximal EQE of as shown in Fig. 7 left), together with AFM images, indicated gradual reduction in the corrugation height as OLED layers were added. The value of *h* in the bare substrate appeared to be *h* ~105 nm, while AFM analysis indicated that *h* ~165 nm. This means that the FIB analysis was done at the features' side, i.e., with the peaks actually representing some point on the slope of the feature. As mentioned, our previous studies [1] indicated that the layer thickness on the slopes is the thinnest. For Substrate A, the reduction in *h* is stronger than observed for devices on substrates with the same period, but larger *h* ~280 to 400 nm. The *a*/*h* ratio for this Substrate A is ~4.5.

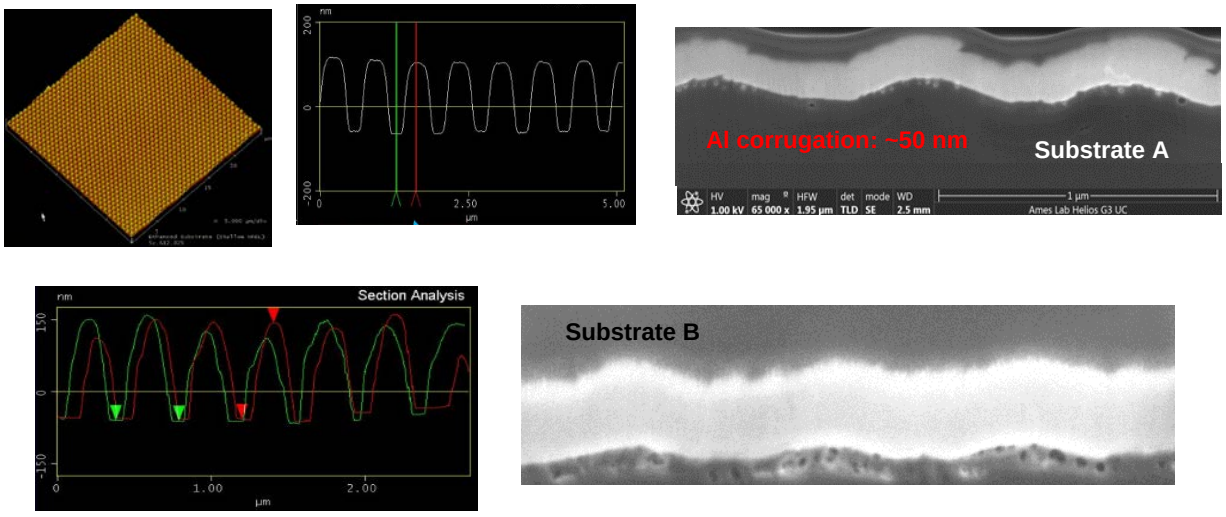

Fig. 14. *AFM analyses of convex PC substrates: Top – Substrate A; 25 μm^2 image (left), and section analysis before (center) PEDOT:PSS application. For this substrate a ~750 nm, and h ~165 & ~125 nm before and after PEDOT:PSS coating, respectively. Based on FIB measurements (right) the corrugation at the top Al was ~50 nm. Bottom - Substrate B with h ~190 nm a ~410 nm before PEDOT:PSS application; after application a remnant corrugation of ~20-30 nm was observed at the Al cathode via FIB (right).*

.

In the case of a white OLED of EQE ~32% (Fig. 8) fabricated on a substrate of *h* ~280 nm & *a* ~750 nm, *h* reduced to ~200 nm at the Al cathode. A similar reduction was observed for a blue OLED (EQE 32.5%) on a substrate with *h* ~310 nm & *a* ~750 nm. Unlike the shallow substrates with low *h* & *a*, as the pitch increase (> 2 μm), and in particular for large *h*, the OLEDs become fully conformal, as seen in Figs. 15 & 16.

Fig. 16 shows a conformal white OLED on concave PET/CAB substrate with *h* ~250 nm and *a* ~2 μm. The OLED is largely conformal up to the Al electrode with some thickness variations across the features**.**

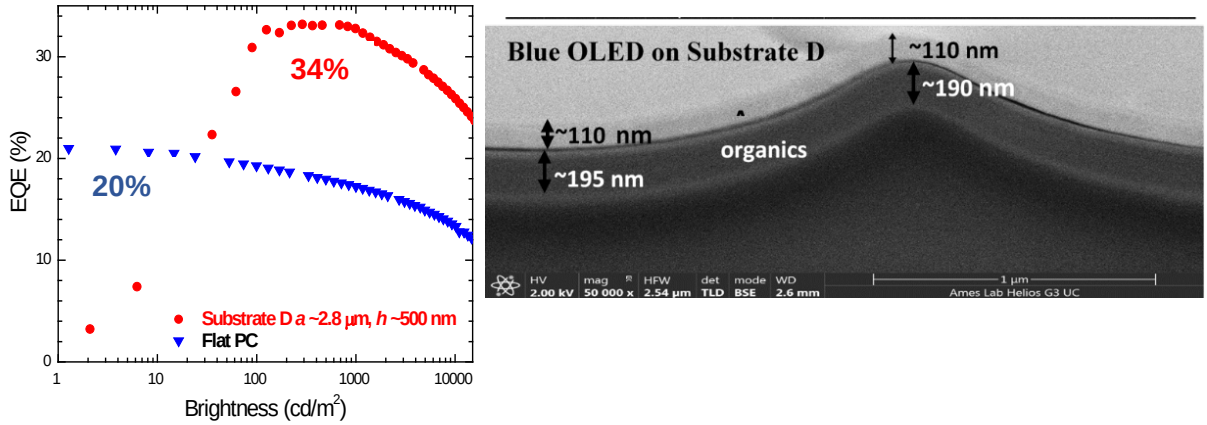

Fig. 15. *Blue OLED on PET/CAB/PEDOT:PSS: h ~500 nm, a ~2.8 μm (see Fig. 1). Fully conformal OLEDs on large–pitch substrates; layers' thickness is as expected from the thickness monitor in the evaporation chamber within the glovebox. EQE ~34%; x1.7 enhancement.*

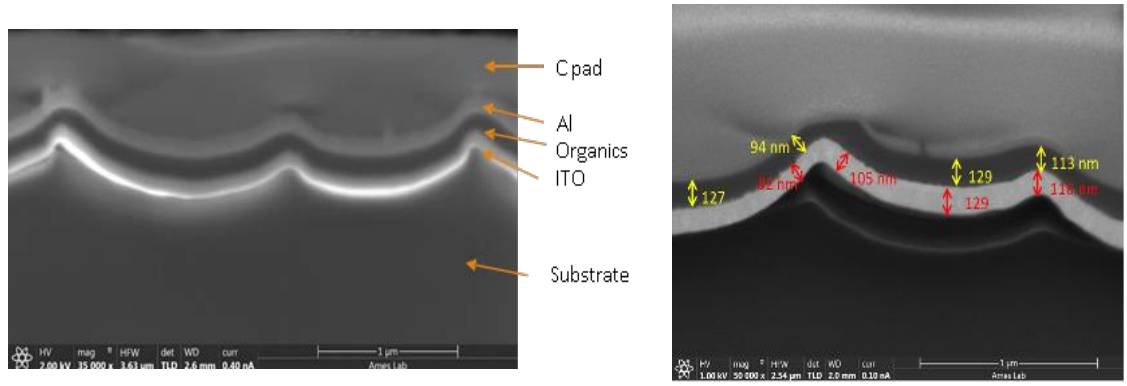

ITO (red arrows); organics (yellow arrows)

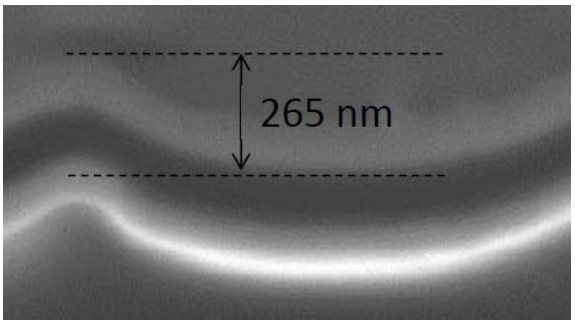

Al layer corrugation

Fig. 16. *Fully conformal white OLED on concave PET/CAB/ITO of h ~250 nm, a ~2 μm.*

Planar OLEDs on planarized buried patterns (MS 5 & MS 10)

As planar OLEDs are preferred over patterned ones, we developed new designs of extraction structures in plastic, generating planarized extracting substrates (PES). The bottom left panel of Fig. 2 above shows our general PES design that consist of an extraction pattern imprinted into a low index polymer planarized by a high index top layer; a general idea first reported in 2014 [2] followed by reports by other groups [3,4]. The adjacent layers are designed with a maximum refractive index contrast. Following optimization, we used a solvent-free Pixelligent (PixNIL) nanoimprintable formulation SFT1, as the use of other formulations that contain solvents resulted in adverse effects on the OLEDs, possibly due to remnant solvent vapor evaporation during the OLEDs' layers thermal vacuum deposition (despite prior baking) that appeared to lead to structural changes. The SFT1 formulation has a refraction index of ~1.9 and is 93% transparent.

As shown below, various low-index pattern geometries were tested to optimize device performance. The PES process is scalable to inexpensive R2R processing and for rigid and flexible glass, as well as barrier-coated plastic substrates.

An external MLA at the substrate's air-side with an index that is matched to or higher than that of the substrate may improve light extraction into air. The MLA can be formed by direct substrate imprinting or by bonding a pre-formed MLA to the substrate.

Our PES substrates differ from conventional planarized designs in a number of important ways, including the ability to form easily and inexpensively a wide range of specific structural shapes in a wide range of materials and with the potential to incorporate commercial barrier films.

Fig. 2 above shows also some examples of PES with additional examples and related attributes shown in Fig. 17, and Fig. 18 shows green OLED attributes fabricated on the PES without added means to extract the externally waveguided photons in the substrate (substrate mode). In addition to OLEDs on Substrate S and Matte, OLEDs on Substrate U (a ~16 μm, h ~4.1 μm) and the planarized close-packed commercial MLA (a ~15 μm, h ~7 μm) are also shown. Following planarization smooth or surfaces with remnant features of ~10 to 40 nm were observed. These however, did not affect the OLED performance. To obtain smoother surfaces we now use a flat glass and roll presser during curing of the applied high-index planarization layer.

As seen in Fig. 18, the EQE of the devices on Substrate S and the commercial MLA were comparable at 30%, compared to a device on glass, where the EQE was ~16%. The EQE of the OLED on the Matte was ~23%. The devices were not encapsulated and as seen next, the addition of IMF between the substrate and the Si PD significantly increased the EQE.

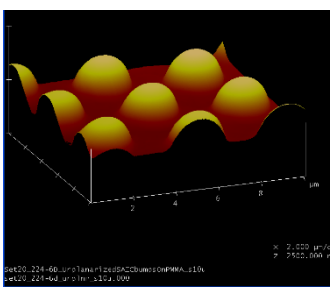

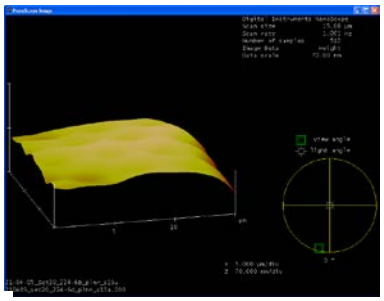

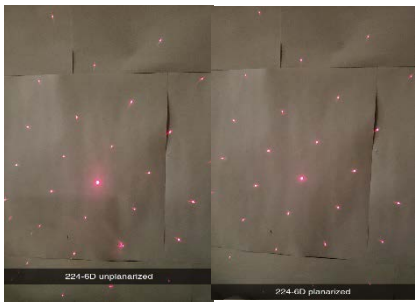

Sample C: *a* ~4 μm, *h* ~1.4 μm

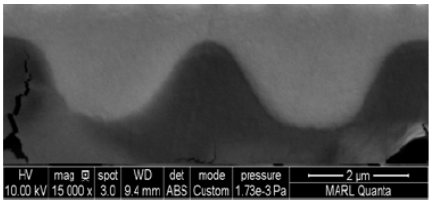

Substrate S: *a* ~4.25 μm, *h* ~1.8 μm

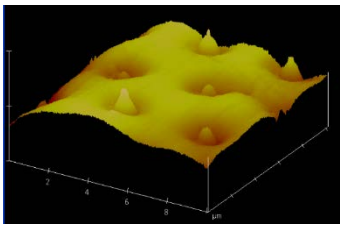

Planarized buried pattern with
up to *h* ~40 nm remnant features.

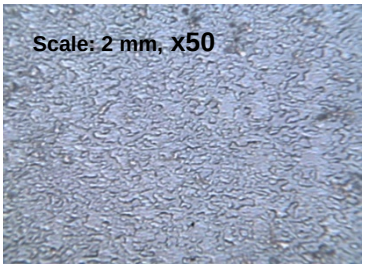

Fig. 17. Top: *AFM and diffraction images of patterned and planarized internal structure in PMMA substrate (Sample C: a ~4 μm, h ~1.4 μm). The roughness of the relatively smooth planar surface was ~10 nm.*
Bottom: Substrate S with remnant surface features (left & center); optical image of the Matte sample with shallow, random features (right).

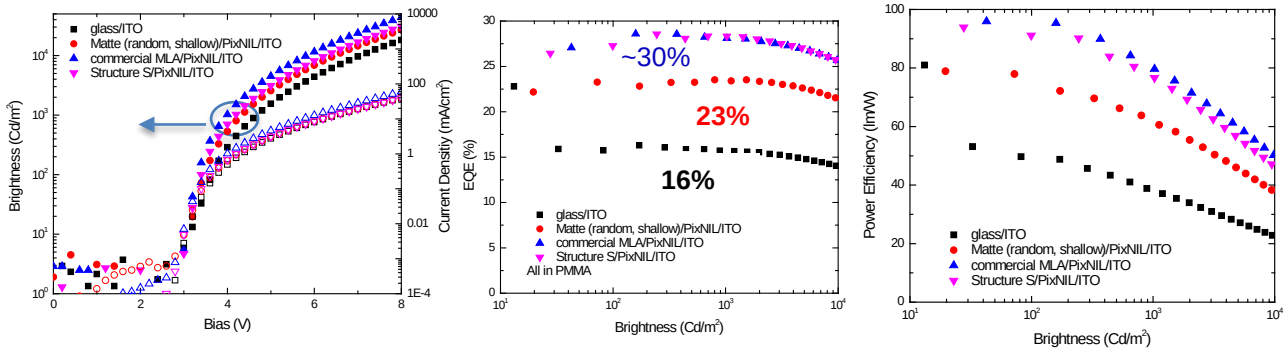

Fig. 18. *J-L-V and EQE & power efficiency vs brightness for green OLEDs on PES Matte, commercial MLA, and Substrate S. ITO was the anode in all cases.*

Fig. 19 shows repeated experiments, where the EQE of a green OLED on Substrate S increased from ~33% to 61% upon extraction of the substrate mode. Devices on reference substrates without a buried pattern are also shown. The substrates include glass/ITO, PMMA/PEDOT:PSS, and PMMA/PiXNIL/PEDOT:PSS; all showed comparable EQEs of ~40%.

Fig. 20 shows two sets of WOLEDs on Substrate S, commercial MLA, and Matte. As seen, the highest EQE of 45.5% was obtained for a WOLED on Substrate S. An EQE of ~40% was obtained for a device on both planarized commercial MLA and Matte. In a separate experiment, Substrates S and U showed comparable EQEs of ~52%.

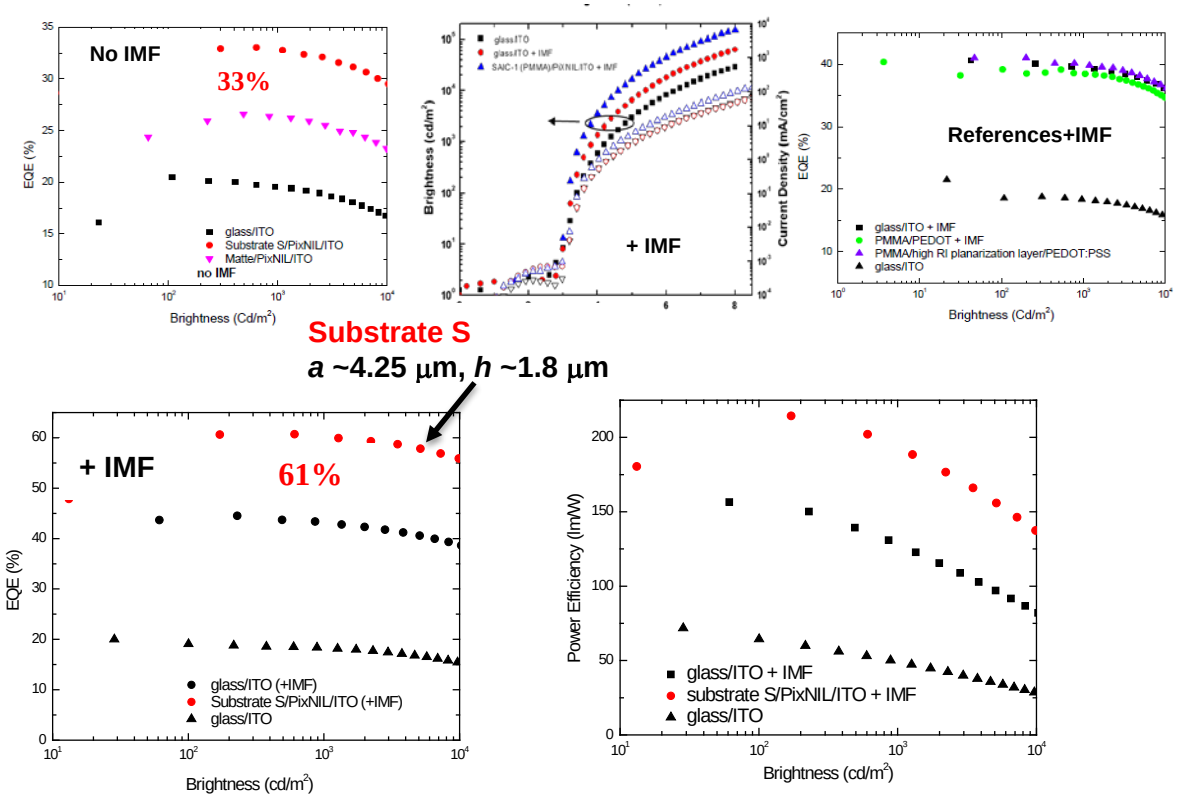

Fig. 19. *J-L-V and EQE & power efficiency vs brightness for green OLEDs on PES Matte and Substrate S with and without IMF. EQE of devices on reference substrates (without a buried pattern) with IMF are also shown.*

In summary, Table 1 summarizes the attributes of successful PES. We obtained comparable EQEs (~55-61%) for planar green OLEDs on both PES with *a* ~4.25 μm & *h* ~1.8 μm (Substrate S) and with *a* ~16 μm & *h* ~4.1 μm (Substrate U); the pitch-to-depth ratios were ~2.4 and 3.9, respectively. Comparable EQEs of up to ~45.5% were obtained also for WOLEDs on the planarized commercial MLA that has a close-packed structure (unlike the other PES) and Substrate S. A maximal EQE of ~52% was obtained for a green device on the shallow, random diffused planarized substrate Matte. Not surprisingly, the OLEDs on the PES with significantly larger pitch-to-depth ratio did not show any enhancement. With optimized WOLEDs, based on three rather than two emitters, we expect to further increase the device efficiency using the structures we designed.

To obtain smoother surfaces we now use a flat glass and roll presser during curing of the applied high-index planarization layer. As shown below, despite these shallow remnant features significant EQE enhancements were obtained with this planarized buried structure.

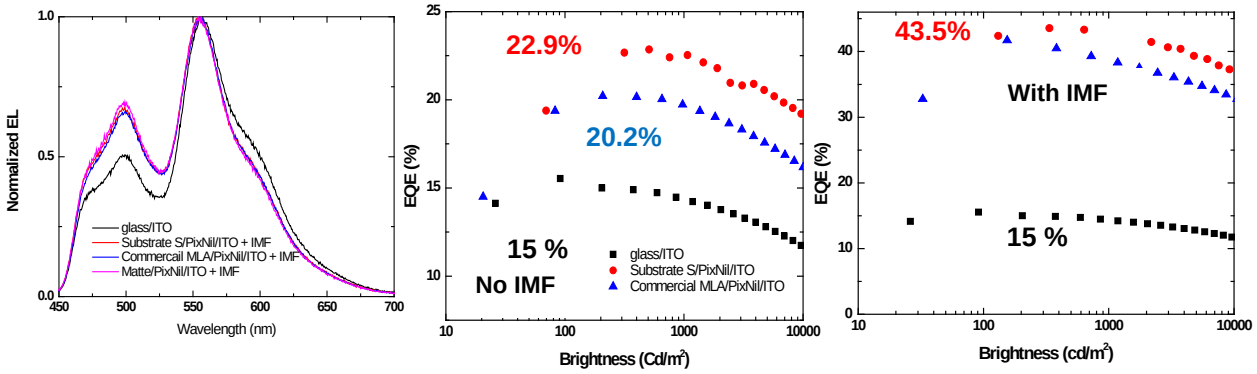

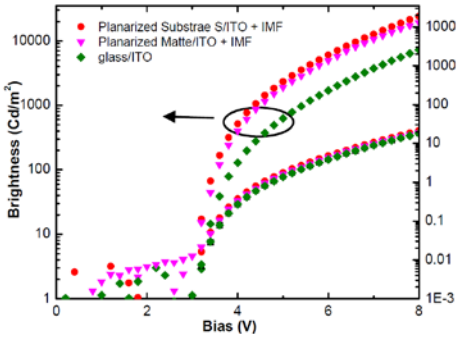

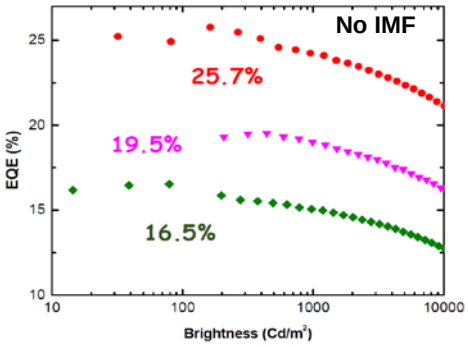

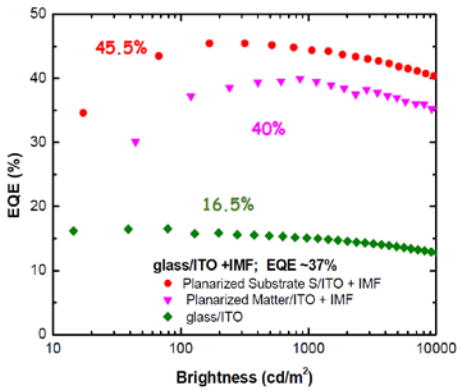

Fig. 20. Top: EL spectra of WOLEDs on Substrate S & commercial MLA and reference substrate and EQEs with and without added IMF. Center and bottom: *J-L-V and EQEs vs brightness for WOLEDs on PES Matte and Substrate S with and without IMF.*

Table 1. Attributes of different successful PES generated in PMMA

Sample	Pitch (μm)	Depth (μm)	Comments & max. EQEs with IMF
Substrate S	4.25	1.8	Shallow remnant features after planarization; ~61% green device & 45.5% WOLED
Substrate U	16	4.1	Smooth surface; generally comparable to Substrate S
Commercial MLA	15	7	Close-packed hexagonal; ~43.5% WOLED
Matte	Random	shallow	Diffuse structure-no regular pattern; ~52% green; ~40% WOLED

Buried periodic planarized structures – simulations (MS 6)

Since the fabricated OLEDs in this project with planarizing extracting substrates (PES) showed large EQE >60%, we performed computational simulations of the simulated the light emission from OLEDs with buried planarized patterns, to determine the ranges of pitch, height and structural parameters that optimize light outcoupling.

The OLED stack we modeled with advanced scattering matrix simulations is depicted in Fig. 21(a); it consists of substrate/planarized corrugations/ITO or PEDOT:PSS Anode/HTL/emissive layer/ETL/cathode. Here, the substrate (refractive index n_1, thickness d_0) has an array of conical features (height d_2). This pattern was planarized with a Pixelligent layer of higher index n_2, which is closely matched to the refractive index of the organic ETL/HTL layers, so that n_2 ~1.8. As in experiments, there is a uniform Pixelligent layer on this pattern (thickness d_2), on which there is an anode (ITO or PEDOT:PSS of thickness d). The HTL (d_3); emissive layer; ETL (d_4) and Ag/Al cathode (d_6) are on the anode. The principal variables in the OLED stack that need to be optimized are the pitch a, and height d_2 of the corrugations, together with the thickness d_1 of the planarizing layer.

In our simulations we utilized a PMMA substrate (n_1 ~1.58) with a Pixelligent planariziring layer (n_2 ~1.8). These results could be readily extended to a Corning willow glass substrate (n_1~1.5). We initially kept the height of the corrugations at d_2 = 1500 nm, typical of the fabricated R2R planarized Microcontinuum structures, and varied a of the corrugation. As described previously, we simulated light emission with parallel component of the wave-vector in the x, y and 45° to the x,y axes - corresponding to the light emission xz, xy and (xy, z) planes, and averaged the three results. By calculating the light emission within the OLED we divided the emission into outcoupled emission to air, substrate modes, and plasmonic losses (Fig. 21).

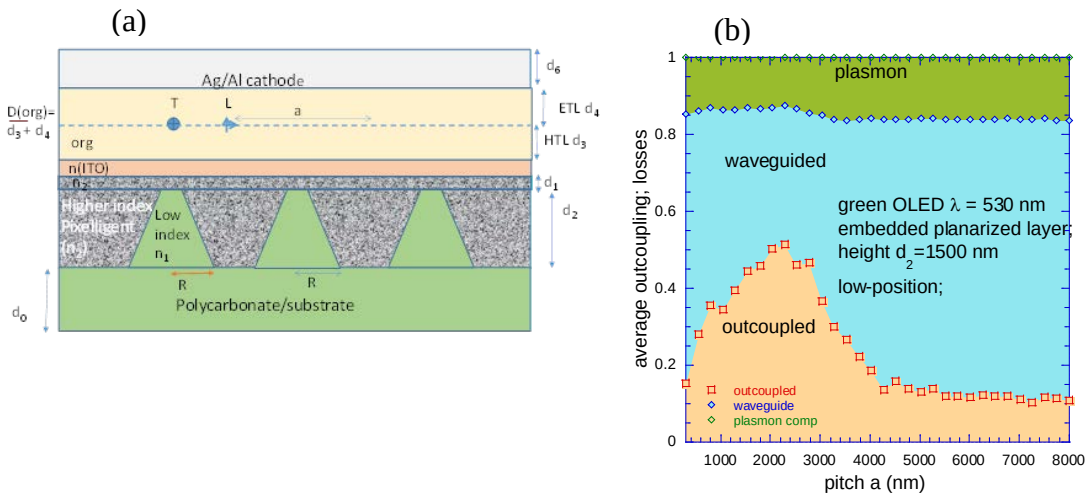

Fig. 21*. (a) Schematic of simulated OLED with buried planarized periodic corrugation layer consisting of a periodic array of substrate cones (pitch a, height d_2, index n_1) that have been planarized by a higher index layer (index n_2). The flat emitting layer between the ETL and HTL is shown by a dashed line. Thicknesses (d_i) of the individual layers are indicated. (b) Division of emitted power into outcoupled power, waveguided power, and plasmonic losses as a function of the a for a green OLED with an embedded planarized layer of height d_2=1500 nm.*

The outcoupled power reaches a maximal value of η_{out} ~50-55% at *a*~ 1-3 μm, after which there is a slow decrease of η_{out} toward the flat limit. The plasmonic losses remain constant at 15-20% for all pitch *a*, since the cathode remains planar. The major sources of losses are waveguided modes in the substrate and higher index layers. The ETL thicknesses are between 50 – 70 nm corresponding to $\lambda/4$ optical thickness, and the plasmonic losses could be reduced by utilizing higher thickness ETL ($3\lambda/4$) or multiple emitting stacks.

` One characteristic feature is the large corrugation height (1500 nm) of the embedded corrugations compared to our earlier conformally corrugated OLEDS (300-500 nm). When a lower corrugation height is used, with d_2 <800 nm for *a* = 2000 nm, or the aspect ratio (d_2/a) of is lower than 0.4, the optimal outcoupling drops rapidly with a large increase in the waveguiding component which exceeds 60% (Fig. 22(a)). At small aspect ratios there is also a modest increase in plasmonic losses as the configuration approaches the planar OLED stack. These simulations indicate that larger aspect ratios >0.5 are necessary to achieve higher outcoupling although there is not significant benefit to increase the aspect ratio beyond 1.

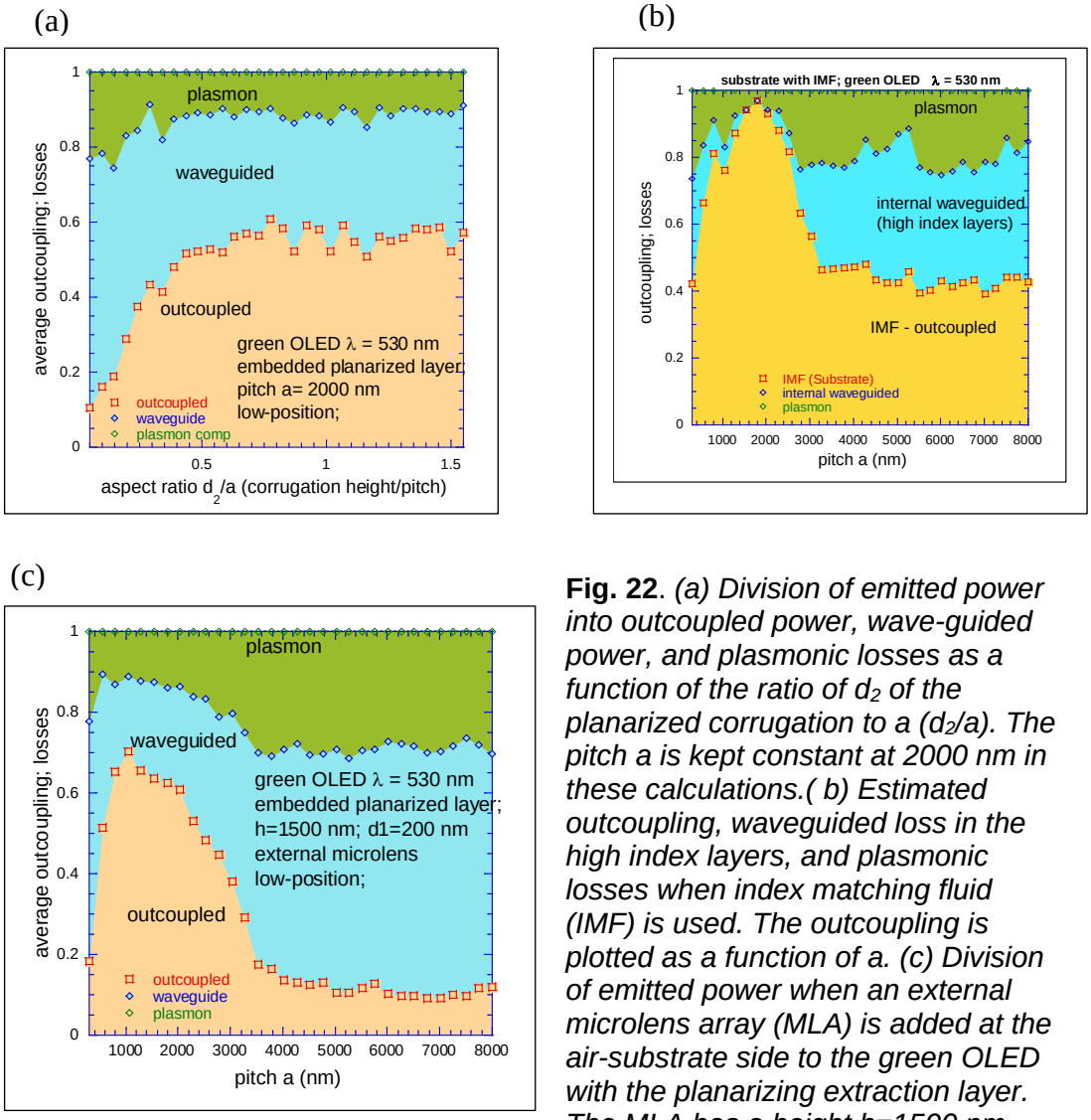

Fig. 22. *(a) Division of emitted power into outcoupled power, wave-guided power, and plasmonic losses as a function of the ratio of d_2 of the planarized corrugation to a (d_2/a). The pitch a is kept constant at 2000 nm in these calculations.(b) Estimated outcoupling, waveguided loss in the high index layers, and plasmonic losses when index matching fluid (IMF) is used. The outcoupling is plotted as a function of a. (c) Division of emitted power when an external microlens array (MLA) is added at the air-substrate side to the green OLED with the planarizing extraction layer. The MLA has a height h=1500 nm.*

Preliminary simulations indicate that results are not sensitive to the thickness of the planarizing higher index layer d_1. Since the measurements achieved high EQE >60% with an IMF, we have developed a scheme to divide the waveguided power into those in the high index layers n ~1.75-1.85), and lower index substrate (n~1.58). Furthermore, we assume that the substrate modes are effectively outcoupled into the IMF. It should be emphasized that there is some overlap of modes between the high index layers and the substrate so that this scheme is an approximation to the actual configuration. This yields a high η_{out} of 80- 90% for smaller a ~2 μm, and substantial outcoupling η_{out} >40%, even for larger pitch a ~8 mm. At larger pitch, substantial plasmonic losses (20%) remain in the substrate accompanied by larger waveguiding loss in the high index layers (Fig. 22(b)).

An external MLA can be attached to the air-substrate side of OLEDs with the PES. We have simulated the MLA has a height h = 1500 nm and the same pitch as the PES. When the a is varied we find that the MLAs increase outcoupling by ~10% relative to the PES without the

MLA, to reach outcoupling of 65-70% (Fig. 22 (c)). Further optimization of the PES and MLA are needed for further OLED improvements.

Complex Substrate Structures (MS 7 & MS 11)

Dual Structures **(MS 7)**
Fig. 23 shows a sketch of dual sided extraction layers formed in a high RI layer. Another example is shown in Fig. 5. As mentioned, while we were able to fabricate such structures they require refinement to enable successful OLED fabrication on them to prevent some area shorts.

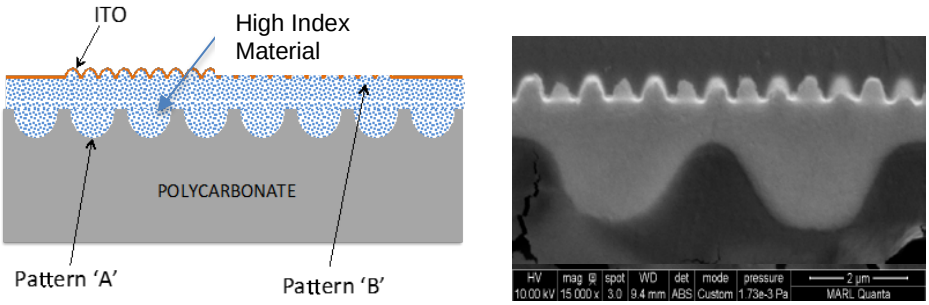

Fig. 23. *Left: Sketch of dual-sided extraction layer formed in high index material (n = 1.70-1.85) with periodic nanoarray on an upper surface and an extracting pattern on the lower surface.*
Right: A fabricated such structure in PMMA with pattern A: a ~4.25 μm, h ~1.8 μm & Pattern B: a ~750 nm, h ~400 nm.

The following sections provide examples of complex substrates (**MS 11**)**.** Various structures of deep or shallow patterns were generated and evaluated. Such structures include dual corrugations, linear patterns, substrates with varying pitch, buckled structures, random patterns, and a hole array. Out of those a random shallow pattern, a buckled structure, and a hole array presented some efficiency enhancement. Figs. 24 - 28 show the structures and some EQE enhancements. Fig. 24 shows a linear array in PET and a substrate with varying pitch generated by applying Ag NW doped PEDOT:PSS to a PC shallow corrugation. Baking at ~70°C and UV irradiating resulted in this structure 'superimposed' on a larger corrugation of *a* ~8 μm and *h* ~100 nm.

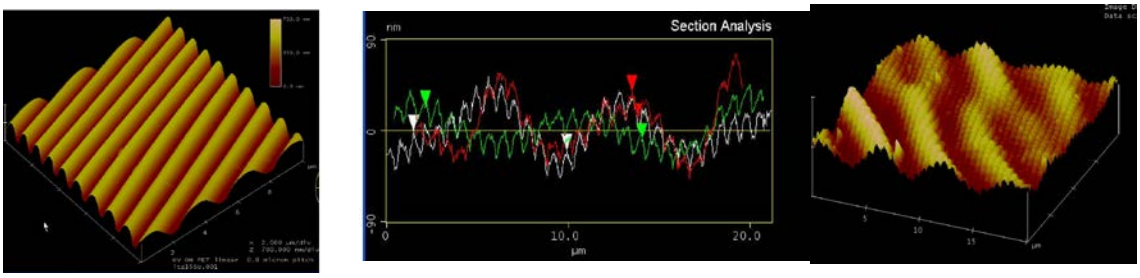

Smooth linearly patterned PET substrate: *a* ~1 μm, *h* ~515 nm.

A PC substrate with a top corrugation *h* ~50 nm & *a* ~750 nm coated with PEDOT:PSS doped with Ag NWs (**MS 3**).

Fig. 24. *A linearly patterned PET (left) and a structure with varying pitch (center & right)*.

Fig. 25 shows a reticulated structure formed due to shrinkage of a specific UV adhesive used in ITO transfer (see Fig. 3) onto patterned convex PET.

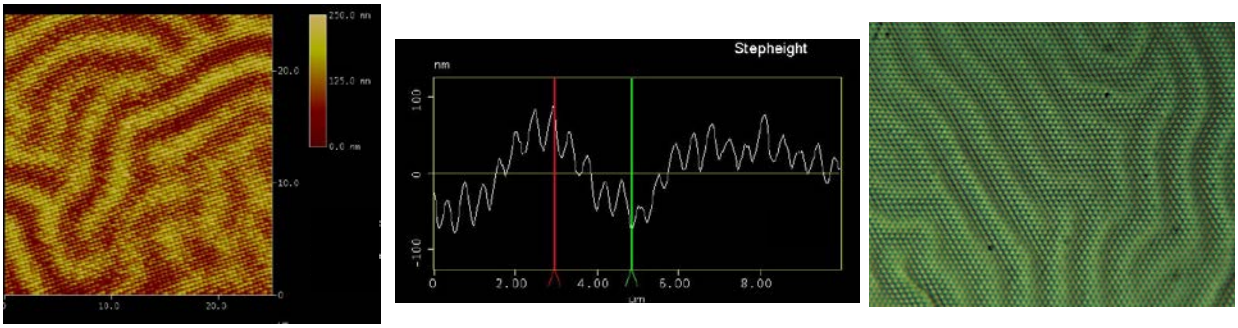

Fig. 25. *AFM (left & center) and an optical pattern (right) of a dual pattern showing a continuous periodic array integrated into a random reticulated pattern. PET/ITO h ~145 nm, a ~415 nm; the secondary pattern is estimated to be of average h ~40 nm.*

Fig. 26 shows random and buckled structures formed via a PEDOT:PSS/Ag NW transfer process. As mentioned, embedding Ag NWs in PEDOT:PSS was studied for improving the conductivity of the PEDOT:PSS anode (**MS 3**), which was indeed achieved. To obtain these multi-period structures we fabricated the anode on polyurethane (PU) via the following transfer process:

- ❑ PDMS was poured over an e.g., PET/CAB pattern.
- ❑ PEDOT:PSS and then Ag NWs were deposited on the PDMS.
- ❑ PDMS/PEDOT:PSS/Ag NWs was next pressed onto PC/PU.
- ❑ Following curing, the PDMS was peeled off.
- ❑ Buckled, multi-period, or random structures were formed.

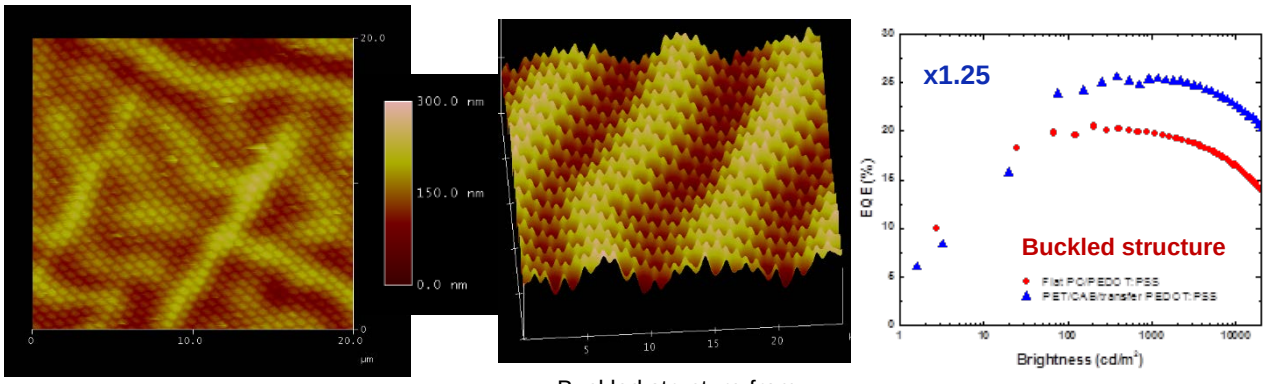

Random structure from patterned PC

Buckled structure from patterned PET/CAB

Red - planar reference OLED
Blue – OLED on buckled PET/CAB substrate.

Fig. 26. *Enhanced EQE for a green OLED on a buckled structure formed by a PEDOT:PSS/Ag NW transfer process.*

Fig. 27 shows an example of a successful planarized extracting structure with and without the addition of IMF to extract the substrate mode (see also Fig. 17) (**MS 12**). Two different pixels are shown, with one of them (Fig. 27 right), but not the other (center), showing micro-shorts at lower current density. The maximal EQE was ~52% with IMF and ~27% without it (the reference device without IMF was of ~20% EQE). The enhanced EQEs with the shallow Matte substrate was surprising.

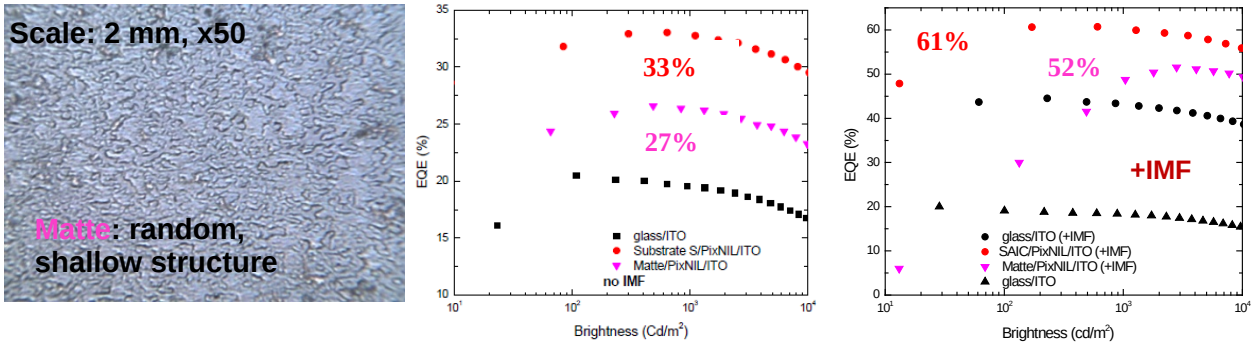

Fig. 27. *Enhanced EQE of a green OLED (without and with IMF) fabricated on a shallow, random Matte substrate, planarized with a high RI layer.*

We developed a new type of buried extraction layer, i.e., a hole array in low-index substrate planarized with a high RI layer**.** An etched Si tool with quasi-random, submicron diameter columns was used to form the extraction structure of ~500 nm dia., ~2-3 μm deep holes planarized with a high-index layer

Fig. 28 shows the tool used for forming the array structure as well as the EQE and power efficiency vs brightness of green OLEDs. An EQE of 23.8% was obtained before extracting the substrate mode. This presents a 40% increase in the EQE. Upon addition of IMF, the EQE was 45%; it increased by 17% relative to planar reference with IMF.

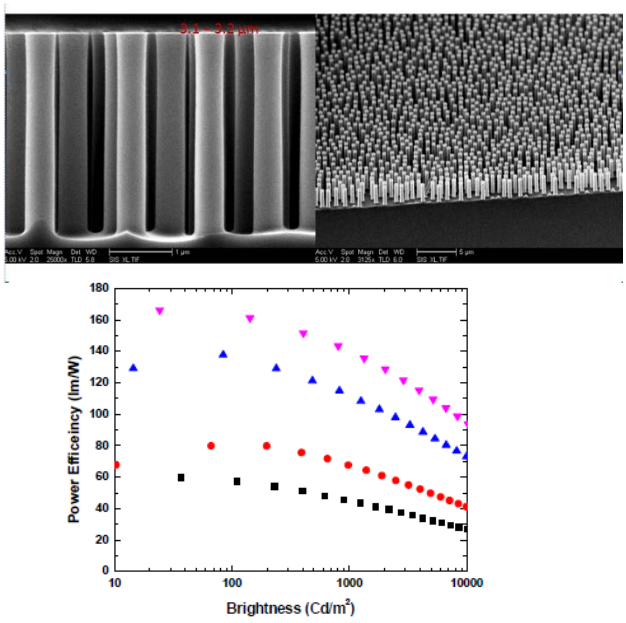

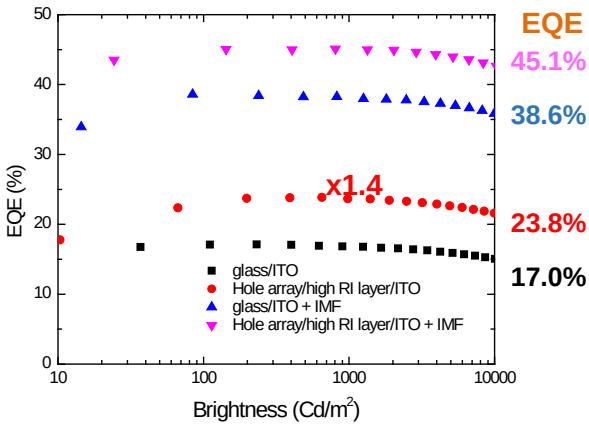

Fig. 28. *Enhanced EQE and power efficiency of a green OLED (with and without IMF) fabricated on a buried hole array planarized with a high RI layer.*

Disordered substrates blue & red OLEDs – Theory

In multi-periodic substrates, there are domains of two different periods a_1 and a_2. The stitching region between the domains may have significant disorder and it is important to assess the contribution of such a region to the light extraction. The light-outcoupling contribution from the disordered region would then be incoherently combined with outcoupling from the periodic domains that we have already studied in the previous project phases.

Previous experimental studies suggest that a feasible way to model the effect of disorder is to consider the reciprocal space of the structure to be dominated by a single ring of reciprocal lattice vectors with magnitude $k=2\pi/l$, where l is the average inter-particle distance in the nanostructure. Accordingly, we model the emission of light from a disordered OLED by considering a dense ring of reciprocal lattice vectors G in a single shell of radius k, to diffract waveguided and surface plasmon modes to the emission cone. Higher-order shells are not included. If we start with a periodic lattice of nanocones and gradually increase disorder – we would retain the first shell of G vectors and further shells would be neglected. The first shell would be decorated with a dense circular array of G vectors, and we divide the first shell of G vectors into N_G uniformly spaced G vectors on the circular shell.

The results of utilizing the first shell of G-vectors with N_G = 110 are shown in Fig. 29. There is little difference in the light emission from xz, yz or the bisector of xz, yz planes, since the G vectors are uniformly arranged on the shell $|G| = 2\pi/l$. The light outcoupling for green emission at 530 nm (Fig. 29) has a maximum of η_{out} ~65-70% similar in value to the periodic corrugation. However the maximum η_{out} occurs for *small* separation values l ~300 nm, significantly smaller than the light wavelength ($l < \lambda$), and $l \sim \lambda/n(org)$. At longer pitch $l > \lambda$, η_{out} drops sharply toward the flat limit at $l > 2\mu$m. The results are very similar for a smaller number $N_G = 73$ G-vectors, indicating reasonable convergence. Since the structure is disordered with a uniform distribution of G vectors in the first shell, we expect a broadband response in the emission over wavelengths. This is confirmed by the results at a blue wavelength of 470 nm (Fig. 29), which is

very similar to the green emission results (530 nm). When the wavelength is increased to red emission (λ = 610 nm) the results are qualitatively similar except that the region of the maximal η_{out} ~65-70% is somewhat broader, spanning separations *l*~400-800 nm rather than the narrower range (400-600 nm) in blue or green OLEDs. The optimal separation *l* is considerably smaller than that for the periodic corrugations (1 -2 μm).

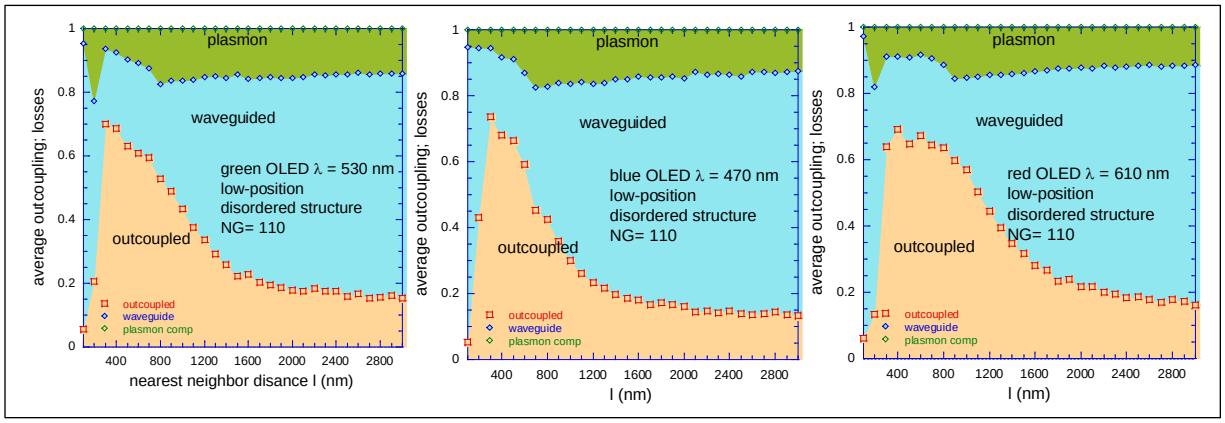

Fig. 29. *Light outcoupling and losses for green, blue, and red OLEDs when a disordered template of nanocones is utilized for the substrate.*

It is of great interest to predict outcoupling from a quasi-periodic OLED structure, which lacks long-range periodicity but has 5-fold or 10-fold rotational symmetry at the lattice sites. Such rotational symmetries are forbidden in crystalline structures. The quasiperiodic structures qualitatively lie between the two extremes of periodic and disordered structures. We calculate the light emission expected from two shells with N_G = 21 vectors, and find a maximal η_{out} ~50-55% for *l*~800-1200 nm, which decreases for larger *l* (Fig. 30). This result is closer to the periodic case although the roll-off in outcoupling is more rapid, than in the periodic case. We do find that η_{out} ~45% with just the first shell of N_G = 11 vectors. A majority of the radiated power occurs in wave-guided modes. These results readily extend to other wavelengths in the visible spectrum in the emission from a blue OLED at λ = 470 nm and a red OLED at λ = 610 nm [5], which show qualitatively the same behavior as the green OLED (Fig. 30). The maximal η_{out} ~50-55% and the roll-off are similar, illustrating broad-band behavior. Although our results are qualitative, they do suggest quasi-periodic templates can enhance light extraction, which may be somewhat smaller than the enhancements for the periodic case. Further calculations are needed to assess the impact of QCs.

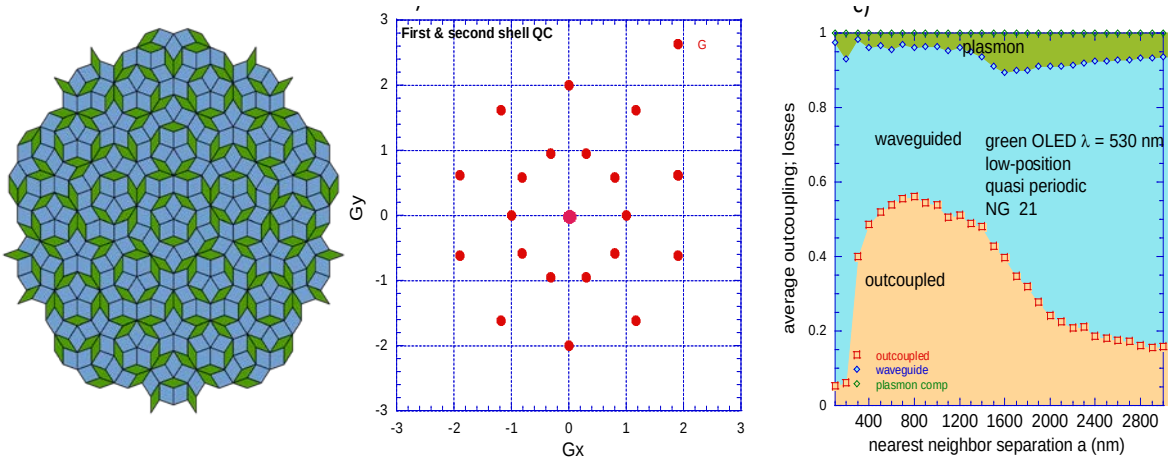

Fig. 30. *(a) Quasi-periodic Penrose tile composed tiling a pentagon and rhombus (b) Schematic depiction of the diffraction spots of a quasi-crystalline structure (c) Outcoupled power and losses for green OLED emission at 530 nm as a function of the nearest neighbor separation l for a simulation with two shells of diffraction G vectors in a quasi-crystalline structure.*

Summary and Concluding Remarks

We designed, fabricated, and evaluated OLED substrates with the goal of maximizing the light outcoupling or extraction factor η_{out} from the resulting OLEDs, i.e., minimizing the losses due to internal waveguiding in the high refractive index (RI) organic+ITO layers and surface plasmon polaritons (SPPs) at the organic/cathode interface.

The substrates were (*i*) smooth convex and concave patterned polycarbonate (PC), polymethyl methacrylate (PMMA), or polyethylene terephthalate (PET)/cellulose acetate butyrate (CAB), and (*ii*) such substrates with an added high RI planarizing layer, i.e., planarized extracting substrates (PES). The substrate fabrication process is amenable to roll-to-roll (R2R) production, which reduces manufacturing costs drastically.

The OLEDs fabricated on these substrates were therefore either (*i*) patterned to various degrees, depending on the pitch *a* and height or depth *h* of the pattern features, or (*ii*) planar, with a pattern buried under the planarizing high RI layer. The substrates and OLEDs were imaged by AFM, and SEM; the latter images were obtained following focused ion beam FIB milling, or via edge SEM.

We demonstrated integrated substrates that included the top pattern, microlens array, and metal mesh/ITO anode with improved plastic/ITO roughness of ~2 to ~3 nm and 25 – 50 Ω/□ sheet resistance.

We demonstrated that the external quantum efficiency (EQE) from green patterned OLEDs reaches ~50% (2x – 2.2x *vs* reference flat plastic/PEDOT:PSS) by mitigating plasmon–related losses and internal waveguiding, even without the addition of a microlens array (MLA), a hemispherical lens, or an index matching fluid (IMF). Simulations conducted in parallel with the experimental effort demonstrated how diffraction by conformally corrugated OLEDs increases

η_{out} to >60%. Structures with varying pitch values were also simulated indicating that outcoupling could reach 60% when averaged over domains of different pitch.

For blue OLEDs EQE reached 34% and for WOLEDs it reached 33% (both 2x *vs* reference plastic/PEDOT:PSS). With an index matching fluid (IMF) EQE reached 61% for green and 45.5% for white OLEDs.

We also evaluated dual and complex patterned substrates, including a promising planarized hole array.

In conclusion, the plastic substrates provide an excellent optimization tool for designs that are cost-effective and compatible with R2R. Moreover, they are transferable to glass. The results we presented with strong theoretical support indicate the capacity to achieve ~70% outcoupling with our metal mesh/ITO integrated PES as well as with an added embedded MLA at the air-side of the substrate.

Combining optimized planarized patterns with embedded air-side MLAs should add at least 10% to the outcoupling. This situation is strongly supported by our new simulations that show an outcoupling of 75% for such OLEDs.

Project Output

Papers

1. Chamika Hippola, Rajiv Kaudal, Eeshita Manna, Teng Xiao, Akshit Peer, Rana Biswas, W. Dennis Slafer, Tom Trovato, Joseph Shinar, Ruth Shinar, Enhanced Light Extraction from OLEDs fabricated on plastic substrates, Adv. Optical Materials 6 (4), 1701244 (2018). https://doi.org/10.1002/adom.201701244.
2. Yu Zhang, Rana Biswas, High light outcoupling efficiency from periodically corrugated OLEDs. ACS Omega **6,** 13, 9291–9301 (2021). (March 23, 2021). DOI: 10.1021/acsomega.1c00903 https://doi.org/10.1021/acsomega.1c00903
3. Yu Zhang, Rana Biswas, Ruth Shinar, Joseph Shinar, Simulation of enhanced light extraction from periodic, disordered and quasi-periodic OLED structures, J. Opt. Soc. Am. B. **38** (9) pp. C144-C152 (2021). DOI: 10.1364/JOSAB.430593 https://doi.org/10.1364/JOSAB.430593 JOSA link
4. Ruth Shinar and Joseph Shinar, **invited review**, Light Extraction from Organic Light Emitting Diodes, under review, *J. Phys: Photonics*, 2022.

Presentations

1. Joseph Shinar,Enhanced Light Extraction from OLEDs fabricated on plastic substrates; an presented at the 2018 Annual SPIE Meeting in San Diego, in the *Organic Light Emitting Materials and Devices XXII.* **Invited talk**
2. Simulations of large enhancement of light out-coupling from periodically corrugated OLEDs, Rana Biswas, Yu Zhang, Iowa State Univ. of Science and Technology (USA) Paper [11093-41]. SPIE Optics and Photonics 2019. Organic and Hybrid Light Emitting Materials and Devices XXIII. Talk on 8/12/2019. https://spie.org/Documents/ConferencesExhibitions/OP19-Final-L.pdf
3. Joseph Shinar, “Organic LEDs (OLEDs): Recent Developments & Current Challenges,” itb Group 2019 Smart Automotive Surfaces Conference, Laurel Manor, Livonia, MI, Oct 9 – 10, 2019. **Invited talk**.
4. Joseph Shinar and Ruth Shinar, “Organic LEDs (OLEDs): Recent Developments & Current Challenges,” 3M Tech Forum, 3M, Maplewood, MN, Dec 2, 2019; **Invited talks**.
5. “Recent results on enhanced light outcoupling from OLEDs on corrugated plastic substrates,” SPIE Conf., *Organic and Hybrid Light Emitting Materials and Devices XXIV*,”

Annual SPIE Meeting, San Diego, CA, August 24 – 28, 2020. Joseph Shinar, Rajiv Kaudal, Erik Dykstra, Michael Fralaide, Yu Zhang, Rana Biswas, W. Dennis Slafer, and Ruth Shinar, Proceedings Volume 11473, 2020. **Invited talk**

Year 1 Milestones

Milestone	Description	Status
MS 1	Smooth Corrugations: design, fabricate; simulations support	*Completed*.
MS 2	Effect of Corrugation Height: achieve EQE ~45%	C*ompleted*. Green OLED EQE: 48% - 50%; Blue and white OLEDs: 32-34% (43.5% WOLEDs on PES +IMF)
MS 3	Anode Improvement: smooth & conductive ITO, + metal mesh	*Completed*. Achieved improved conductivity and smooth ITO (~2-3 nm roughness on PC, ~25-50 Ω/□); delivered metal mesh buried in ITO*
MS 4	Air-side Extraction:	*Completed*. Fabricated microlens array directly on the air-side of flat and corrugated substrates. Fabricated buried MLA.**
MS 5	High Index Corrugation; (partial) planarization EQE 50%	*Completed*. Corrugation was flattened as proposed using Norland and Pixelligent high-index layers; there was significant improvement with added IMF. >60% (green OLED>60%; WOLEDs 43.5%).
MS 6	Initial Simulation of Non-Periodic Structures:	*Completed*. Main work was performed in Year 2. Simulations of disordered and quasi-periodic structures yielded outcoupling >50%

* Issues of OLED shorts with the buried mesh in a pattern. Need to evaluate direct ITO deposition over the metal mesh versus ITO transfer conditions.

** MLAs are less efficient than IMF at the substrate/Si PD interface.

Year 2 Milestones

Milestone	Description	status
MS 7	Optimized WOLEDs/single-period substrates. Continue to optimize metal mesh/ITO & MLA in dual patterned (periodic) substrates: test also on green OLEDs. EQE ~50%	*Achieved* EQEs of ~50 -60% for corrugated green OLEDS and devices on high RI planarized buried patterns. For WOLEDs – 43.5%
MS 8	Complex Corrugations: simulations to guide experiment in single-period, multiple-period & (qausi-) random substrates with variable patterns	*Completed.* Designs with >60% outcoupling predicted
MS 9	Stacked Tandem OLEDs: begin fabricate tandem cell on planarized and corrugated substrates. Evaluate single color devices & WOLEDs + OLEDWorks EQE ~55%	MCI is developing polymer-to-glass pattern transfer process without moisture/O_2 leakage pathways for OLEDWorks substrates.
MS 10	Conformality evaluation of multi-stack patterned OLEDs on various substrates	*Completed*. Effect of *h* & *a* elucidated.
MS 11	Complex Corrugation Device Fabrication: commence fabrication on multi-period, etc. substrates	Tested a variety of complex structures with some structures showing improved EQEs (hole array and Matte). >50% for green OLEDs
MS 12	Air extraction on the most promising substrates, including with complex designs EQE ~65%	*Achieved* >60% EQE for green OLEDs, but only with use of IMF.
MS 13	Fully integrated substrates/devices with EQE ~70% (see micrograph of metal mesh embedded in high RI planarized extraction substrate)	Integration of the mesh/ITO is more promising with the planarized buried structure. With improved OLEDs, we expect EQEs of ~70%

References

1. C. Hippola, R. Kaudal, E. Manna, T. Xiao, A. Peer, R. Biswas, D. Slafer, T. Trovato, J. Shinar, and R. Shinar, “Enhanced Light Extraction from OLEDs Fabricated on Patterned Plastic Substrates,” *Adv. Opt. Mater.* **6**, 1701244 (2018).
2. J.-W. Kim et al., “FDTD analysis of the light extraction efficiency of OLEDs with a random scattering layer,” *Optics Express* **22**(1), 498 (2014)
3. H. Cho et al., “Organic wrinkles embedded in high-index medium as planar internal scattering structures for organic light-emitting diodes,” *Org. Electr.* **46**, 139 (2017)
4. Y. Qu et al., “Efficient, Nonintrusive Outcoupling in Organic Light Emitting Devices Using Embedded Microlens Arrays,” *ACS Photonics* **5**, 2453 (2018).
5. Y. Zhang et al., “Simulation of enhanced light extraction from periodic, disordered, and quasi-periodic OLED structures,” *J. Opt. Soc. Am. B* **38**, C144 (2021).